LAPPEENRANTA UNIVERSITY OF TECHNOLOGY

School of Energy Systems

Energy Technology

Sergio Rafael Martinez Orozco

MOTOR TYPES COMPARISON DETERMINING EFFICIENCY IN PUMPING SYSTEMS

Master's thesis

2015

Examiners: Professor D.Sc. Jero Ahola, D.Sc. Tero Ahonen

Supervisor: D.Sc. Tero Ahonen

Abstract

Lappeenranta University of Technology

LUT School of Energy Systems

Degree Programme in Electrical Engineering

Sergio Rafael Martinez Orozco

Motor Types Comparison Determining Efficiency in Pumping Systems

Master's thesis

2015

79 pages, 40 figures, 9 tables

Examiners: Professor D.Sc. Jero Ahola

D.Sc. Tero Ahonen

Keywords: pumping system, electric motor, efficiency map, variable speed drive, energy savings

Pumping, fan and compressor systems consume most of the motor electricity power in both the industrial and services sectors. A variable speed drive brings relevant improvements in a fluid system leading to energy saving that further on can be translated into Mtons reduction of CO_2 emissions.

Standards and regulations are being adopted for fluid handling systems to limit the less efficiency pumps out of the European market on the coming years and a greater potential in energy savings is dictated by the Energy Efficiency Index (EEI) requirements for the whole pumping system and integrated pumps. Electric motors also have an International Efficiency (IE) classification in order to introduce higher efficiency motors into the market.

In this thesis, the applicability of mid-size common electric motor types to industrial pumping system took place comparing the motor efficiency characteristics with each other and by analyzing the effect of motor dimensioning on the pumping system and its impact in the energy consumption.

Acknowledgements

Table of Contents

Abbreviations and symbols

Roman letters

$\hat{A}$	Peak current density	[A/m]
B	Magnetic flux density	[V s/m^2]
$\hat{B}$	Peak magnetic flux density	[V s/m^2]
E	Electric field strength	[V/m]
f	Frequency	[Hz]
F	Lorentz force	[N], vector
H	Head	[m]
i	Electric current	[A]
$\vec{\imath}_s$	Stator current space vector	
j	Imaginary unit	
l	Length	[m]
L	Characteristic length	[m]
L	Inductance	[H]
L_m	Magnetizing inductance	[H]
L_σ	Leakage inductance	[H]
n	Shaft speed	[rpm]
p	Number of pole pairs	
$p\Omega$	Rotor angular speed	[rad/s]
P	Power	[W]

Q	Electric charge	[C]
Q	Flow rate	[liters/s]
r	Radius	[m]
R	Resistance	[Ω]
t	Time	[s]
T	Electromagnetic torque	[Nm]
u	Voltage	[V]
v	Speed, velocity	[m/s]

Greek letters

β	Angle	[°], [rad]
δ	Air gap (length)	[m]
η	Efficiency	[%]
θ	Angle	[°], [rad]
τ_p	Pole pitch	[m]
Ψ	Magnetic flux linkage	[V s]
Ψ_m	Magnetizing flux linkage	[V s]
ω	Angular speed, angular frequency	[rad/s]

Subscripts

d, D	Direct axis component
e	Electromagnetic
m	Magnetic
q, Q	Quadrature axis component
r	Rotor
s	Stator
δ	Air gap

Acronyms

AC	Alternating Current
BEP	Best Efficiency Point
DC	Direct Current
EEI	Energy Efficiency Index
EEM	Energy-Efficient Motor
EPA	Extended Product Approach
ErP	Energy-related Products
EU	European Union
FEM	Finite Element Method
HEV	Hybrid Electric Vehicle

IEC	International Electrotechnical Commission
IM	Induction Motor
IPMSM	Interior Permanent Magnet Synchronous Motor
IRR	Internal Rate of Return
LSPM	Line Started Permanent Magnet motor
MEI	Minimum Efficiency Index
NEMA	National Electrical Manufacturers Association (United States)
OEM	Original Equipment Manufacturer
PM	Permanent Magnet
PMSM	Permanent Magnet Synchronous Motor
PMASynRM	Permanent Magnet-Assisted Synchronous Reluctance Motor
SynRM	Synchronous Reluctance Motor
VSD	Variable Speed Drive

Chapter 1

1 Introduction

1.1 Background

The European Union (EU) industrial sub-sectors, such as non-metallic minerals, paper, pulp, print, chemical, iron-steel and machinery-metal cover almost three quarters of the total industrial electricity consumption in the EU [1]. The majority of the motor electricity consumption takes place in pumps, fans and compressors, representing more than 60% in the industrial sector and more than 80% in the services sector as shown in Fig 1.1and Fig 1.2 respectively.
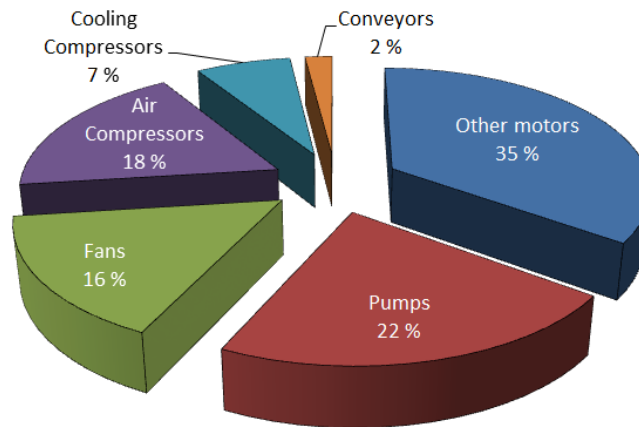

Fig 1.1 Share of motor electricity consumption by type in the industrial sector.
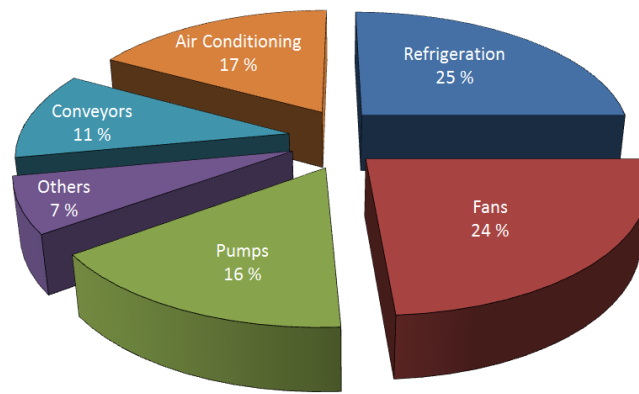
Fig 1.2 Share of motor electricity consumption by type in the services sector.

Energy-Efficient Motor (EEM) applications such as efficient pumps, fans and compressors may lead to electricity savings and in consequence, to economic savings in both the industrial and the services sectors. Improvements on the components, design and system operation can be done in order to increase efficiency, but especially with the usage of Variable Speed Drives (VSD) and their controllability, where lies the largest energy saving potential; however, their usage and application within Europe has been limited due to certain obstacles such as split budgets, lack of internal incentives and the high initial cost. An estimated value of the economic savings potentials was obtained, being 45 TWh for the industrial sector and 9 TWh for the services sector [1].

Electricity savings along with the implementation of EEM and VSD would translate into MTons reduction of CO_2 emissions. In some situations, this type of drives for speed control is not so economically attractive in the services sector, where their initial cost is still elevated. One of the reasons is that VSD are more efficient in higher power operation range, where the number of operating hours is significantly higher.

Water pumps are a part of many electric motor systems (see Fig 1.3 for an industrial pumping system). This type of pumps is being part of a recent study from the European Commission together with stakeholders in order to analyze the technical, environmental and economic aspects of water pumps. The mentioned study shows that water pumps are widespread within the European Union and it is predicted that by 2020 their annual energy consumption will reach 136 TWh [2].
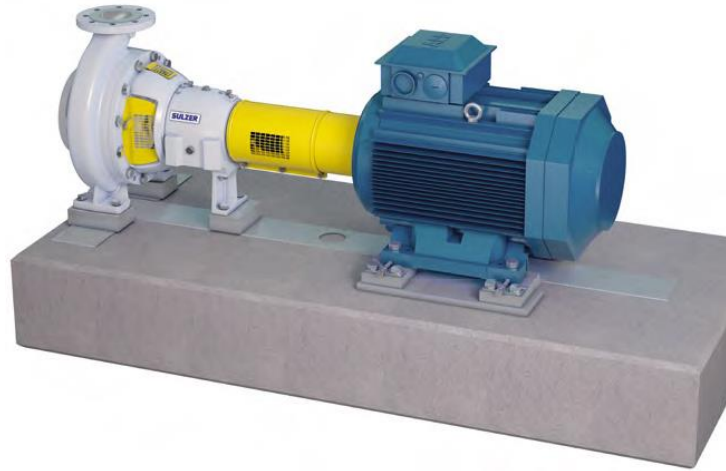
Fig 1.3 Typical industrial pumping system installation.

Due to this share of total electricity consumption, there have to be improvements by means of new technologies that will be able to reduce both purchase and operation costs in water pumps. To achieve those improvements, some standards and regulations are being adopted in order to increase the market diffusion of technologies that enhance the life-cycle environmental impact of water pumps. One important part of the previously mentioned regulations is the Minimum Efficiency Index (MEI), which is a dimensionless scale unit for hydraulic pump efficiency at 75%, 100% and at 110% (overload) of the BEP. The MEI value ranges from 0 to 1; a lower value means the less efficient pump. The MEI by January 2013 was 0.1 (the lowest 10%) and starting in January 2015 it should be at least 0.4 (the lowest 40%), the benchmark for the most efficient water pumps is MEI=0.7 at the time of developing the directive. This index regulation limits the water pumps with less efficiency in the whole European market for the coming years [2].

However, the European Association of Pump Manufacturers (Europump) is aiming for a greater energy saving potential of approximately ten times bigger than the current regulations for water pumps, using a methodology called Extended Product Approach (EPA) to calculate the Energy Efficiency Index (EEI) of the components of certain product

(pump, motor or VSD) and also for integrated units. The EEI calculation of fixed speed pumps and variable speed pumps will be evaluated according to reference control curves and load profiles. Since EEI considers the applied flow control methods, it provides the energy efficiency requirements and the expected future requirements for the whole system that need to be adopted in the coming years [3].

One clear example of the so called 'next generation' pumping systems can be obtained from circular pumps that must be controlled by a VSD and are now regulated by the EEI. Such pumps can be built in small dimensions, for example the Grundfos MAGNA3, which is constructed with a permanent magnet synchronous motor and integrated VSD (Fig 1.4).

Fig 1.4 MAGNA3 high-efficiency pump cutaway.

The MAGNA3 is an enhanced version of pumping systems with circulators and nowadays is considered as a brand new concept for industrial pumping systems, it is being produced by the Danish company Grundfos. It has a full range of high-efficiency circulators for heating, cooling, ground source heat pump systems and domestic hot water applications. The main features are corrosion protection, perfect insulation, clamp ring, Neodymium technology rotor, compact stator, air cooling in control box, integrated sensors and high-quality user interface [4].

Another manufacturer that keeps innovating in the water pumping systems industry is Xylem with its brand named Flygt. The main Flygt Experior characteristics are speed regulation, self-cleaning functionality, premium efficiency motor, simplified user-friendly control and longer bearing and motor lifetime, which makes the pump, motor design and VSD very reliable [5]. This wastewater pump (Fig 1.5) includes Hard-iron impellers for highly abrasive and corrosive water handling. It implements a Line Started Permanent Magnet motor (LSPM), that has been investigated for instance by Tanja Heikkilä [10] that uses less current and make the pump more slender and lighter.

Fig 1.5 Flygt Experior wastewater pumping system.

The previously mentioned couple of pumping systems differ a lot compared with the typical industrial pumping systems in terms of design. In the typical cases, the centrifugal pump is coupled to an induction motor that may have a separate frequency converter and their components can be obtained from different manufacturers, which lead to a possible extra energy consumption since the devices are not optimized to interact with each other. Many considerations should be taken into account to match the electrical characteristics of the motor and frequency converter to avoid the possibility of premature failure of the pumping system [13]. The main advantage of the industrial pumping systems is the

capability of replacement of broken devices. At first instance, the pump and motor have their own bearing construction and the frequency converter has to be manually configured by the user.

1.2 Motivation for the study

One important part of any pumping system in terms of their construction is the motor type that can be included, which may be chosen from different designs such as an Induction Motor (IM), Synchronous Reluctance Motor (SynRM), Permanent Magnet Synchronous Motor (PMSM) and Permanent Magnet-Assisted Synchronous Motor (PMASynRM). Their main characteristics and construction will be analyzed in the next chapter together with the equation model for these types of motors.

Some other criteria are also worth to mention, giving a high importance to the information related to the costs that all of the different kind of pump configurations involve, their maintenance and lifetime concerning both the customer and the manufacturer perspectives.

1.3 Objectives

To define the most energy efficient and versatile electric motor type for a 15 kW Close Coupled Pump running at rated speed of 1500 rpm. The term versatility, in this case for an electric motor, refers mainly to the dimensions that can be selected freely by the end-user (height and principally the length), to the weight limitations regarding the motor construction, and it also refers to the air ventilation that can be integrated in the machine.

To estimate the energy savings potential comparing different types of motors is also considered as part of the objectives.

Figure 1.6 is an example, but not limited to a Close Coupled Pump to be analyzed [18], which involves an impeller in the same shaft as the electric motor that drives the pump. The pump itself does not have a separate coupling, saving money and time-consuming operations. These characteristics among others, makes this type of pump simple and available at a relatively low cost.

Fig 1.6 Close Coupled Pump.

An aluminum frame is ideal for motors in pumping applications and its inclusion has increased over the past decades. Some advantages of this material are the dimensional stability (to avoid warps and cracks), lighter weight (between 15% and 45%) translated into lower costs, and improved heat dissipation, compared to a cast iron frame. New aluminum alloys also bring high corrosion resistance and tensile strength [19].

Chapter 2

2 Motor comparisons and indicative results

2.1 Principles of electric motors

The force applied by the magnetic field on a charged object or a current-carrying conductor can be calculated with the usage of the Lorentz force, which is considered as a force experienced by an infinitesimal charge dQ moving at a speed v. The vector equation below describes that force:

$$dF = dQ(E + v \times B) = dQE + \frac{dQ}{dt}dl \times B = dQE + idl \times B \qquad (2.1)$$

This basic vector equation is fundamental when computing the torque for electrical machines, especially in the latter part of the equation, where a current-carrying element of a conductor of length dl is considered [8].
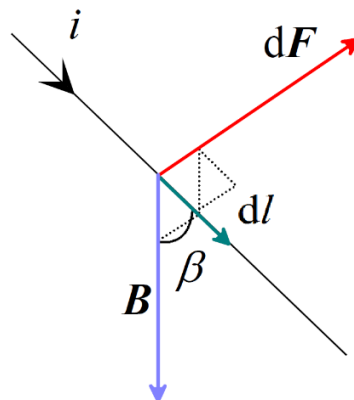
Fig 2.1 Application of the magnetic part of the Lorentz force to a current-carrying conductor.

Fig 2.1 shows the Lorentz force dF acting on a differential length dl of a conductor carrying an electric current i in the magnetic field B. The angle β is measured between the conductor and the flux density vector B. The vector product i dl x B may now be written in the form i dl x $B = i$ dlB sinβ. The force dF is perpendicular to the plane conformed by dl and B according to the right-hand screw rule. The maximum value of dF is reached when dl and B are perpendicular, in other words, sin$\beta = 1$.

In an electrical machine, an air gap flux density B_δ that penetrates the rotor surface, intersecting the current-carrying rotor bars, generates a tangential force on the periphery of the rotor, as illustrated in the figure below:
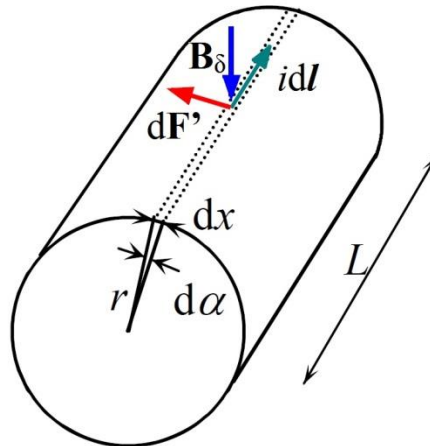
Fig 2.2 Lorentz force acting on the rotor surface.

Fig 2.2 shows a current element of the width dx on a rotor surface. Also, the air gap flux density B_δ is present acting upon that surface. The force dF' and the rotor dimensions such as radius and length are also illustrated.

Now we consider as sinusoidal both the flux density distribution and the linear current density distribution and assume the magnetic flux direction perpendicular to the rotor

surface. Line integrating the Lorentz force dF around the surface of the rotor and multiplying by the rotor radius, we obtain the electromagnetic torque equation, in this case, for a two-pole machine [11]:

$$T_e = r \int_0^{2\pi} F = r\hat{A}\hat{B}\tau_p cos\theta \tag{2.2}$$

where r is the rotor radius, $\hat{A}$ is the peak current density in the conductor, $\hat{B}$ the peak magnetic flux density and τ_p the pole pitch. The electromagnetic torque can be shown in a vector form if the equation 2.2 is analyzed with the usage of the space vector theory, which is very useful for advanced control tasks. This results in the following general equation:

$$T_e = \frac{3}{2}p(\vec{\psi}_m \times \vec{\imath}_s) \tag{2.3}$$

where p is the number of poles, $\vec{\imath}_s$ the stator current space vector and $\vec{\psi}_m$ the magnetic flux linkage of the air gap. It has to be taken into account that both the flux linkage and the current have to be always in the same voltage level and most of the time referred to the stator winding.

2.2 Motor types under study and their construction

The main property of rotating electric machines is the transformation of mechanical energy into electrical energy and vice versa. There are lots of industrial processes where the electricity produced comes from these electrical machines; however, a relatively small portion of electricity producing processes prescinds from the usage of rotating machines and in that case, auxiliary motors are needed to fulfill the energy requirements [8].

Regarding the global electricity production, near half of it is being used in electric motors and the demand of controlled drives applications is growing considerably, since the control of torque must be accurate, those drives may save big amounts of energy.

There are two main categories of electric motors and they rely on the type of electric system to which the motor is connected, one of them is the direct current (DC) motors and the other is alternating current (AC) motors. One advantage of AC motors against DC is the lower maintenance requirement. Motors with alternating current supply are divided in two subcategories: synchronous and asynchronous motors. The speed of the rotor matches the speed of the magnetic field in the case of a synchronous machine, while the speed does not coincide in the case of an induction machine [7]. A figure of the basic construction of an AC motor is shown next, describing the main parts that conforms the machine (Fig 2.3).
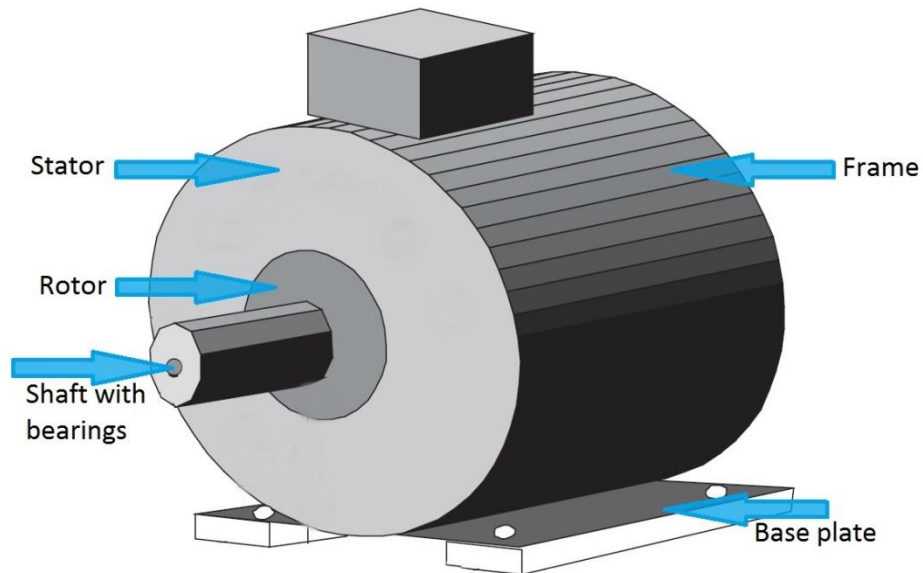

Fig 2.3 AC motor basic construction

Now an in-depth image shows the stator construction, which is made up of many thin laminations of cast iron or aluminum. They are perforated and clamped together to form the

stator core in shape of a hollow cylinder with slots. Coils of insulated wires are inserted into these slots and each group of coils forms a pair of poles. The number of poles depends on the internal connection of the stator windings. A three-phase winding is placed and arranged in the stator core slots to create a rotating magnetic field (Fig 2.4).
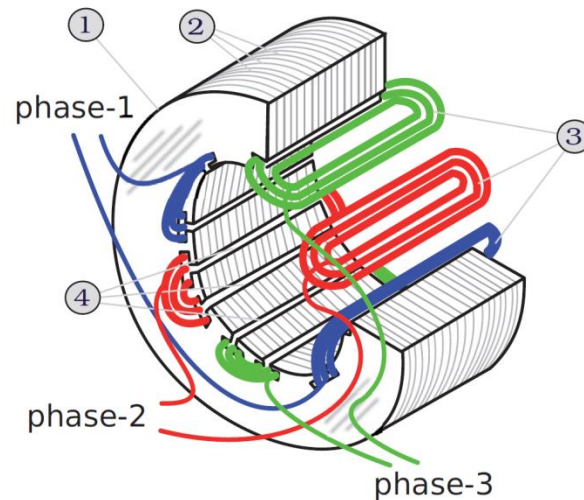
Fig 2.4 Detailed stator construction of an induction machine.

1. Stator core   2. Steel laminations   3.Winding   4. Slots

Transient states are present in electrical machines in the start-up and through some parts of the process control, either fed by a frequency converter or by a sinusoidal supply. There are equivalent circuits for motors in both the stationary and the transient state, but the last one needs to be analyzed with the help of different techniques, one of them is the Space Vector Theory, where the next assumptions are made with the aim of simplify the analysis:

- Flux density distribution in the air gap is considered as sinusoidal.
- Saturation of the magnetizing circuit is assumed constant.
- Iron losses are neglected.
- Inductances and resistances are independent of the frequency and temperature.

As an example, the equivalent circuit of an induction motor is shown in Fig 2.5. It has a reference frame rotating at speed ω_g. The voltages u and currents i are vectors, the flux linkages ψ are also vectors. The angular frequency ω_g is not present in the stator reference frame [11].
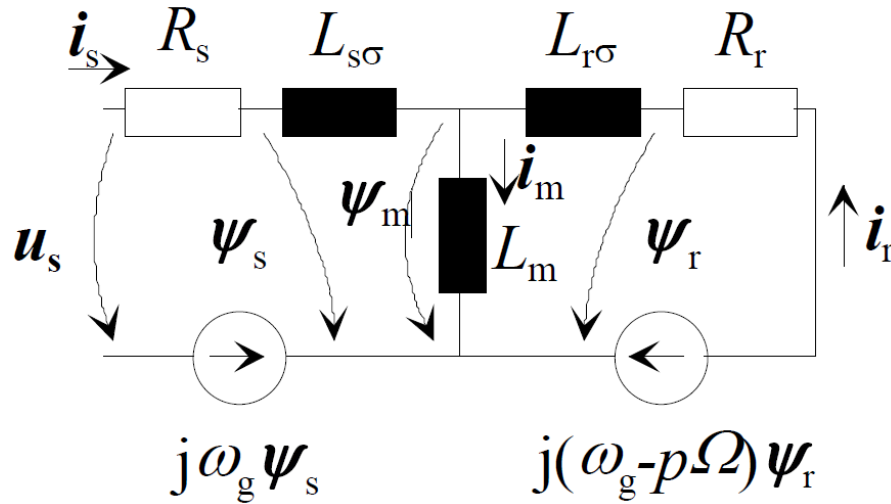
Fig 2.5 Equivalent circuit of an induction motor based on Space Vector Theory.

From now on, the voltages and flux linkages can be represented with the following equations. At first instance, the voltage equations 2.4 and 2.5 must be set in a general frame of reference and rotating at an angular speed ω_g. The additional motion voltage term $j\omega_g\psi_{s/r}$ is applied to these equations whenever the observation frame of reference rotates.

$$u_s = R_s i_s + \frac{d\psi_s}{dt} + j\omega_g\psi_s \tag{2.4}$$

$$u_r = R_r i_r + \frac{d\psi_r}{dt} + j(\omega_g - p\Omega)\psi_r \tag{2.5}$$

where $p\Omega$ is the rotor electrical angular speed, also indicated as ω_g. The flux linkages occurring in equations 2.4 and 2.5 are represented in the equations below:

$$\psi_s = L_s i_s + L_m i_r \tag{2.6}$$

$$\psi_r = L_r i_r + L_m i_s \tag{2.7}$$

where L_m is the magnetizing inductance, L_s is the total inductance of the stator (calculated as $L_m + L_{s\sigma}$) and L_r is the total inductance of the rotor ($L_m + L_{r\sigma}$). $L_{s\sigma}$ and $L_{r\sigma}$ are the leakage inductances of the stator and rotor, respectively. The magnetizing flux linkage is thus a product of the varying inductance and the current [11]:

$$\psi_m = L_m(i_s + i_r) = L_m i_m \tag{2.8}$$

In the coming sections of this chapter, four different types of AC motors are being studied (IM, PMSM, SynRM and PMASynRM) by meanings of their construction (weight and components), efficiency and equation models. Besides this, a comparison is done including different applications where these types of motors appear.

2.2.1 Induction Motor

Induction motors have been present in the industrial sector for several years and still are the preferred and most used electric machine type due to its simple construction that brings high reliability, their robustness and also to the low manufacturing and maintenance costs [9]. There are two types of induction motors: single-phase and three-phase. The first one is fed by single-phase power supply and its pulsating magnetic field is produced by the stator winding. Household applications are the most common usage for this type of induction motor, such as refrigerators, fans, washing machines, coolers, etc.

On the other hand, the three-phase induction motor is fed by three-phase power supply and the present rotating magnetic field is produced by the stator windings. Their application focuses in industrial drives like pumps, drills, stamping presses, metal cutting machine

tools, conveyors, etc. At the same time, three-phase induction motors are divided in two different kinds: squirrel cage rotor and wound rotor [7].

In terms of construction (Fig 2.6), the stator is the fixed part of the motor, which is a hollow laminated cylinder, also called a stator core, with axial slots on its inner surface. Said core is made of steel laminations, insulated each one from another. The rotor is the rotating part of the motor and is settled inside the stator. The rotor is a laminated cylinder (rotor core) with axial slots on its outside surface, winding and the shaft. It is also built with insulated steel laminations. An air gap is present between the stator and the rotor.

Motor bearings are also an important part of the construction of a machine because they provide a reduction of the rotational friction and support for both radial and axis loads. There are different types of motor bearings depending on the application and their selection must be carefully taken into account. The most common type is the deep groove ball bearing, suitable for high speeds due to their low frictional torque. Cylindrical roller bearings, sleeve bearings and angular contact ball bearings are other types among the available variety on the market nowadays [14].
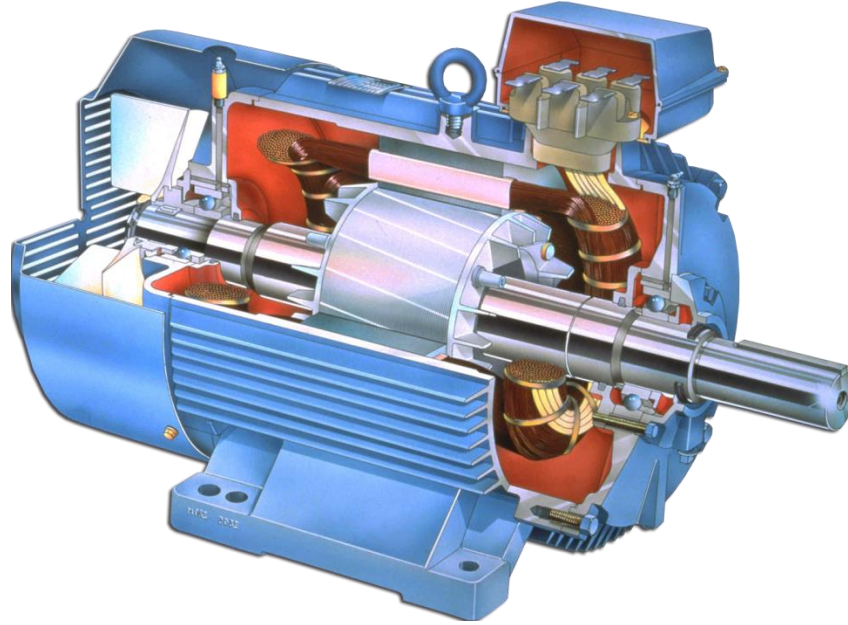
Fig 2.6 Induction motor construction overview.

As already mentioned before, the construction of the stator is practically the same in all AC motor types; however, the difference resides on the rotor composition where we can find two types as seen previously: squirrel cage rotor and wound rotor (also known as slip-ring rotor). The first one possesses bars short-circuited at each end by two rings (Fig 2.7).
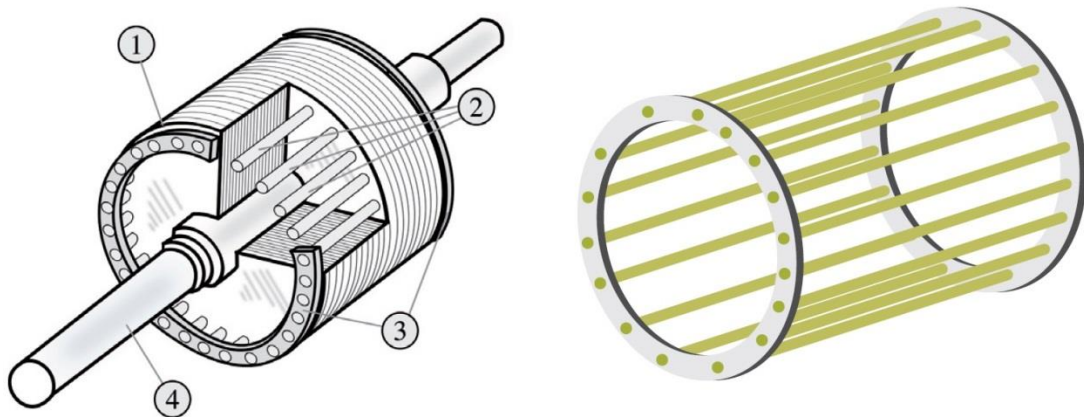
Fig 2.7 Detailed squirrel cage rotor construction and winding.

1. Rotor core   2. Bars   3. End rings   4. Shaft

When there are two squirrel cages, one inside the other, both windings are independent and this kind of rotor is known as double cage (Fig 2.8). This type of rotors is rarely used in the industry; their main application is for producing NEMA C characteristics, which require a high starting torque with low starting current. They are more expensive than class A and B designs that are meant to have a normal starting torque and current. Double cage rotors are used for high starting torque loads, such as loaded pumps, compressors and conveyors [15].
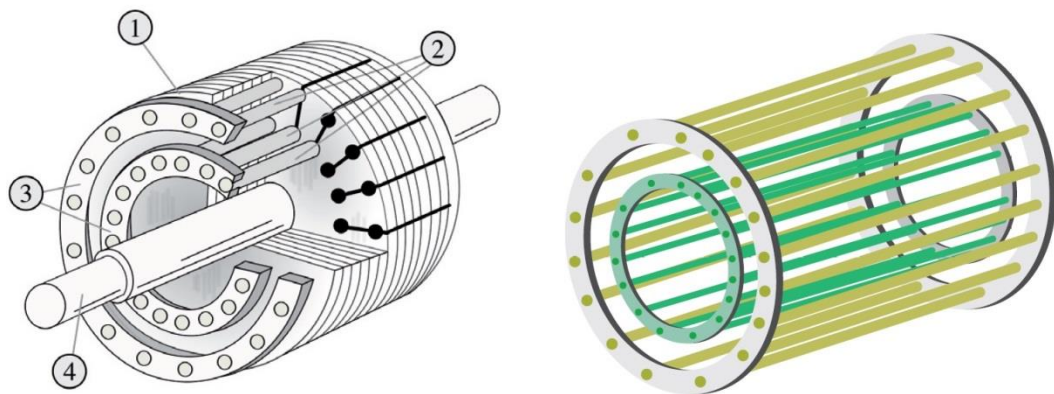
Fig 2.8 Detailed double squirrel cage rotor construction and winding.

1. Rotor core   2. Bars   3. End rings   4. Shaft

In the case of a wound rotor, the winding is made of coils; each one consists of several insulated wire turns. When connected in series, these coils form a coil group. In the simplest form, a three-phase winding has three coil groups and each group has up to one coil. Hence, the three identical coils have a 120 electrical degrees phase shift. Wound rotor has a complicated design that in consequence increases the costs and decreases the reliability. That is why this type of rotor will not be analyzed further in this paper. Nowadays it is used just in a few applications that require heavy starting duty and also in some drivers that need speed control [7].

Torque production and equation model for an Induction Motor.

The induction motor can be represented in an equivalent circuit based in the rotor reference frame as shown in the figure below:
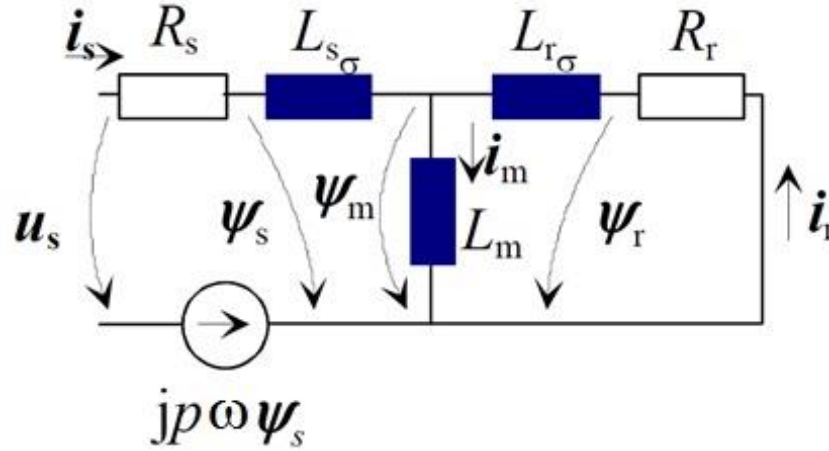
Fig 2.9 Asynchronous machine equivalent circuit.

After some steps and mathematical manipulation, the general equation for torque (eq. 2.3) can be seen in terms of the stator current space vector and rotor flux linkage space vector:

$$T_e = \frac{3}{2}p(\psi_s \times i_s) = \frac{3}{2}p\frac{L_m}{L_r}(\psi_r \times i_s) \tag{2.9}$$

$$T_e = \frac{3}{2}p\frac{L_m}{L_r}(\psi_{rd}i_{sq}) \tag{2.10}$$

where ψ_{rd} is the flux and i_{sq} the torque producing components. It is important to notice that there is no quadrature component in the rotor flux linkage reference frame. The angular frequency is considered as $\omega=2\pi f$. At this point, it is possible to transform the machine equations from the rotor to the flux linkage frame with a few trigonometric functions from the known parameters:

$$sin\theta_{\psi\text{d}} = \frac{\psi_{\text{rq}}}{\sqrt{(\psi_{\text{rd}})^2+(\psi_{\text{rq}})^2}} = \frac{\psi_{\text{rq}}}{\psi_{\text{r}}} \quad , \quad cos\theta_{\psi\text{d}} = \frac{\psi_{\text{rd}}}{\psi_{\text{r}}} \tag{2.11}$$

Now the torque can be expressed based on the cross field principle:

$$T_{\text{e}} = \frac{3}{2}p\frac{L_{\text{m}}}{L_{\text{r}}}\left(\psi_{\text{r}\psi}i_{\text{sT}} - \psi_{\text{rT}}i_{\text{s}\psi}\right) = \frac{3}{2}p\frac{L_{\text{m}}}{L_{\text{r}}}\left(\psi_{\text{r}\psi}i_{\text{sT}}\right) \tag{2.12}$$

As mentioned before, there is no quadrature component here; this is the reason of the simplicity of the equation. The torque control is made by manipulating i_{sT} which is perpendicular to the rotor flux linkage [11].

2.2.2   Permanent Magnet Synchronous Motor

Like in the squirrel cage motor, the stator of a Permanent Magnet Synchronous Motor (PMSM) includes a normal three-phase winding, but the difference is noticed in the rotor construction, where the winding is replaced with permanent magnets, hence, a rotor flux coupling always exists. The magnets can be mounted on the surface or embedded in the rotor.

The quality of the permanent magnet materials plays an important role in the motor performance; poor quality magnets may limit the motor control considerably. On the other hand, high quality permanent magnet materials are being developed and manufacturers keep launching PMSM since they have been available for a long time, but nowadays enhanced version of machines with those high quality magnets. For example, the wind mill generators are pointing to the usage of permanent magnet machines [11].

In terms of the physical construction, the rotor of a permanent magnet machine can be built of electric sheet, like the case of an asynchronous motor and of course different types of lamination exist with the aim of giving the desired characteristics of the machine. The stator of a permanent magnet machine is quite similar to the one of an induction machine. Fig 2.10 shows the cutaway diagram of the permanent magnet synchronous machine. More details about the rotor construction can be seen later in this section.
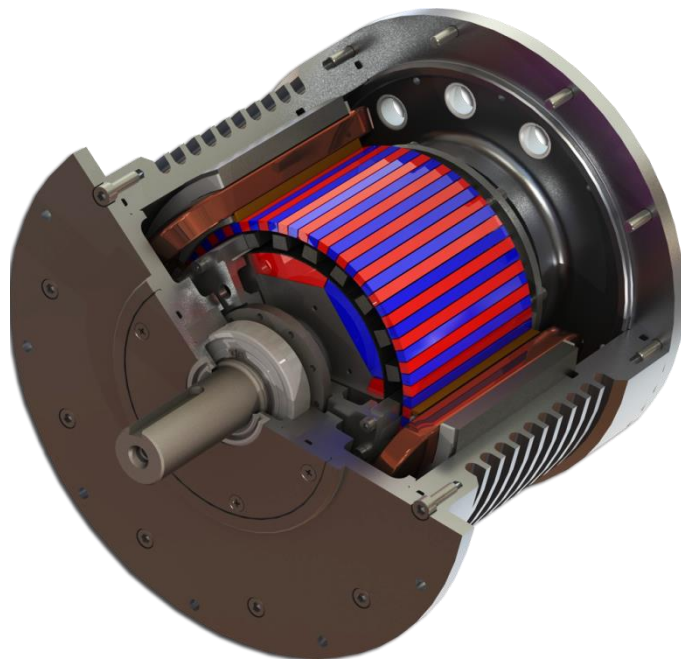
Fig 2.10 Permanent Magnet Synchronous Motor construction overview.

The usage of magnets in the machine, either embedded or surface mounted in the rotor, provides unique characteristics since the permanent magnet material is indeed part of the magnetic circuit of the machine, which leads to an impact or influence on the reluctance. Control methods in PMSM vary depending on the position of the permanent magnets in the rotor and they require information on the rotor angle. The magnets can be located in a different array in the rotor as shown in Fig 2.11. They can be glued on the rotor surface or

embedded partly or completely into the rotor. According to the resulting ratio of the direct and quadrature inductances, the PMSM may be classified as a salient pole machine when $L_d > L_q$.
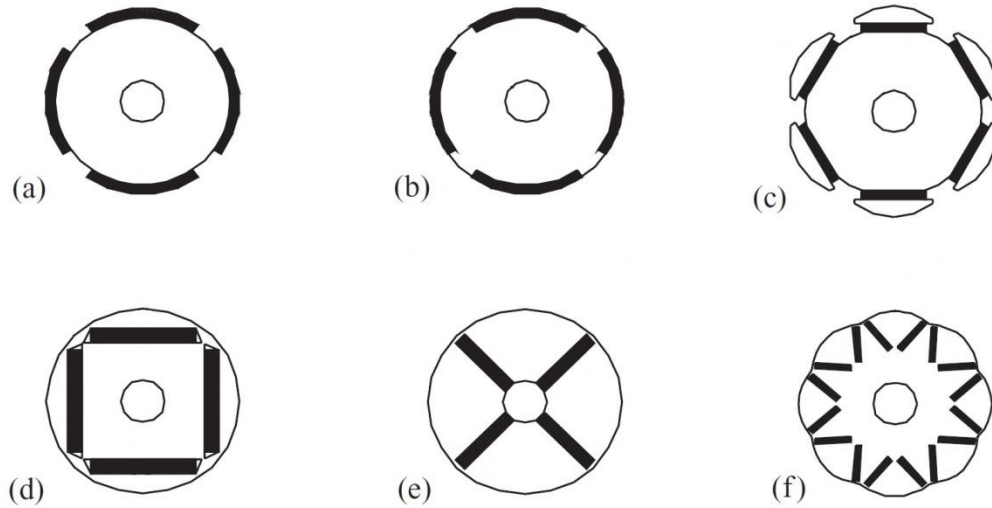
Fig 2.11 Permanent Magnet Synchronous Machine rotor types.

a) Surface mounted   b) Embedded   c) Pole shoe

d) Tangentially embedded   e) Radially embedded   f) V-shaped

Peculiarly in the surface mounted case (Fig 2.11a), the magnet material is used in the best possible way since its high magnetic circuit reluctance produces low synchronous inductances and in consequence, the machines built with this rotor type produce the highest pull-out torque. When the magnets are embedded in the rotor surface (Fig 2.11b), a reluctance difference exists and the maximum produced torque can be reached at a pole angle above 90 degrees because the inductance in the q-direction is slightly higher than in the d-direction.

In Fig 2.11c the rotor plates shape resembles the construction of a salient-pole machine where a sinusoidal flux density is achieved in the air gap and a smooth and quiet operation is achieved at a low rotation speed. In addition, the poles are designed to obtain a sinusoidal form in the flux and at the same time to reduce the magnetic leakage on the machine. The rotor of the machines from Fig 2.11d and e gives the motor a hybrid property because it behaves somehow as a SynRM without magnets. The torque is produced by the different inductances in both the direct and quadrature directions. In fact, the resulting torque is known as reluctance torque. Adding the magnets to this hybrid machine results in improvements at start-up, also the efficiency and power factor are considerably better than in the SynRM.

In the case of V-shaped magnets (Fig 2.11f), two magnets are used per pole and it is possible to get a high air gap flux density in no-load conditions. The number of pole pairs is usually high because the thickness of the stator yoke (meaning the stator surface) is reduced and therefore a larger rotor diameter exists in the machine [8].

Torque production and equation model for a Permanent Magnet Synchronous Motor.

The equivalent circuits of a PMSM are obtained analyzing the machine with direct and quadrature reference frame fixed to the rotor. Those circuits can be seen in Fig 2.12.
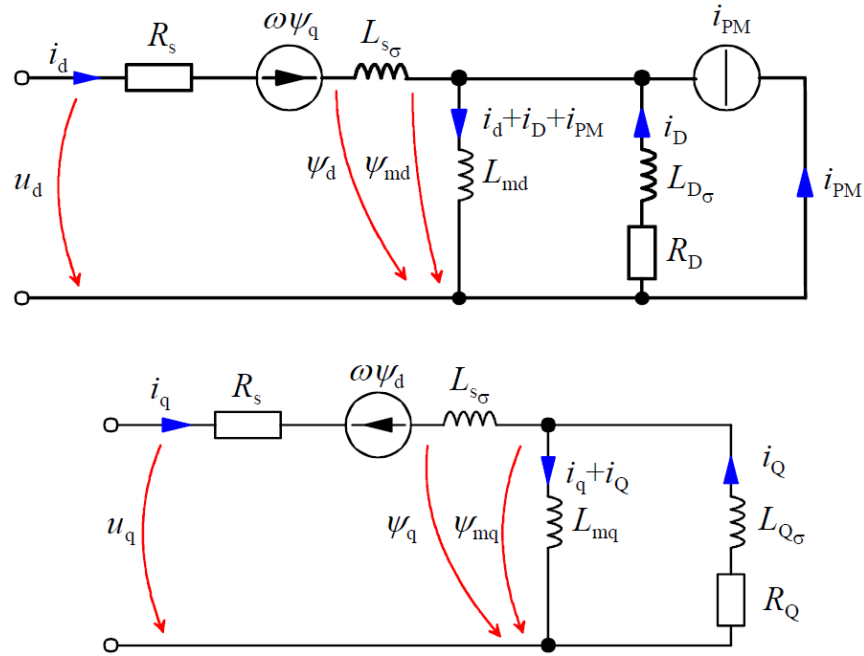
Fig 2.12 Permanent Magnet Synchronous Machine equivalent circuits in d and q directions.

In the figure above, i_{PM} represents the permanent magnet as a current source in the rotor circuit. This current source creates the permanent magnet's share of the air gap flux linkage in the magnetizing inductance: $\psi_{PM} = i_{PM} L_{md}$.

It was previously seen that the voltages can be represented in a motor equivalent circuit by equations 2.4 and 2.5 (in the general form). Those equations now specified for a PMSM in the rotor reference frame are shown below:

$$u_{sd} = R_s i_{sd} + \frac{d\psi_{sd}}{dt} - \omega\psi_{sq} \tag{2.13}$$

$$u_{sq} = R_s i_{sq} + \frac{d\psi_{sq}}{dt} + \omega\psi_{sd} \tag{2.14}$$

$$0 = R_D i_D + \frac{d\psi_D}{dt} \tag{2.15}$$

$$0 = R_Q i_Q + \frac{d\psi_Q}{dt} \tag{2.16}$$

The flux linkage components can be obtained with the coming equations:

$$\psi_{sd} = L_{sd}i_{sd} + L_{md}i_D + \psi_{PM} \tag{2.17}$$

$$\psi_{sq} = L_{sq}i_{sq} + L_{mq}i_Q \tag{2.18}$$

$$\psi_D = L_{md}i_{sd} + L_D i_D + \psi_{PM} \tag{2.19}$$

$$\psi_Q = L_{mq}i_{sq} + L_Q i_Q \tag{2.20}$$

The field current generates a flux linkage in the permanent magnet:

$$i_{PM} = \frac{\psi_{PM}}{L_{md}} \tag{2.21}$$

Nevertheless, the field current i_{PM} is not constant; this is due to the saturation of the magnetizing inductance L_{md} which produces the permanent magnet's share of the air gap flux linkage.

Using the cross-field principle, the torque equation can be obtained. Torque is a starting point for the development of many control principles of a PMSM:

$$T_e = \frac{3}{2}p\left[\psi_{PM}i_{sq} - \left(L_{mq} - L_{md}\right)i_{sd}i_{sq} + L_{md}i_D i_{sq} + L_{mq}i_Q i_{sd}\right] \tag{2.22}$$

The first term $\psi_{PM}i_{sq}$ depends on the flux linkage of the permanent magnets and on the stator current perpendicular to the flux linkage. The second term $\left(L_{mq} - L_{md}\right)i_{sd}i_{sq}$ could be of high importance if the saliency ratio in the d and q axes is large. The third and fourth terms are related to the torque components of the damper windings, they only occur during transients [11].

2.2.3   Synchronous Reluctance Motor

Along with the permanent magnet motor, the Synchronous Reluctance Motor (SynRM) has been gaining a place in the market. One of the main reasons is the convenient properties they offer, and another reason is that the developing of an induction machine cannot go any further, despite of being the most inexpensive industrial motor type.

The SynRM is also a three-phase electric motor with the attribute of having the rotor construction in a peculiar way, where the measured values vary depending on the direction. Electric steel plates are stacked together forming the rotor structure. Those plates have punched holes that act as flux barriers.

The torque produced in a SynRM is proportional to the difference between the d and q axes inductances, bigger difference means more torque production. The direct axis is built with magnetically conductive material (iron in the majority of cases) and the quadrature axis is designed with magnetically insulating material (air) [11]. Fig 2.13 shows an example of the construction for the reluctance machine.

Fig 2.13 Synchronous Reluctance Motor construction overview.

The aim of the construction of the rotor in a SynRM is to keep the saliency ratio as large as possible. This ratio takes into account the direct axis inductance L_d and the quadrature axis inductance L_q. The saliency ratio mainly determines the peak torque of the machine, power factor and the maximum possible efficiency. If we compare a SynRM with an IM of the same size, the saliency ratio of the synchronous reluctance motor should be at least ten to make it competitive against the induction motor.

The rotor of a synchronous reluctance machine has many different types of construction and in hence, the saliency ratio varies from one to another. These rotor types are shown in Fig 2.14 and explained briefly afterwards.
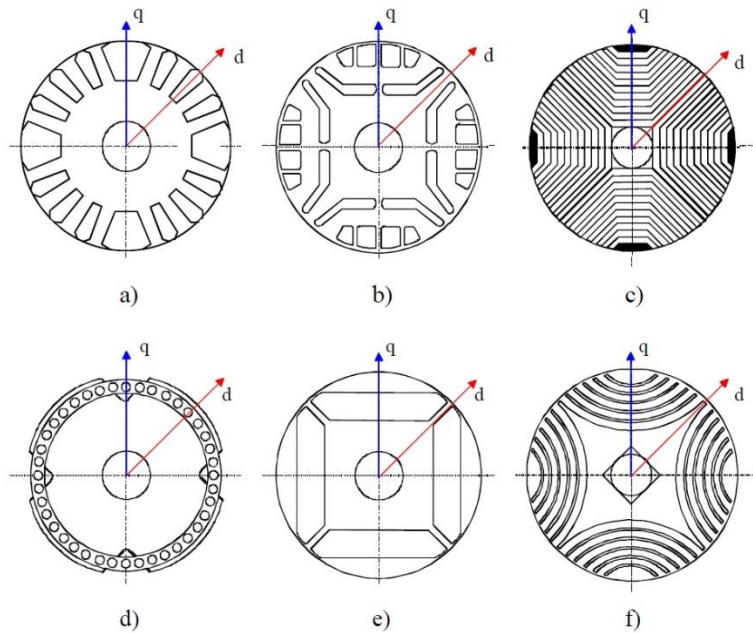
Fig 2.14 Synchronous Reluctance Machine rotor types.

If some of the teeth from the rotor of an IM are removed, the most simple structure for a SynRM can be obtained as can be seen in Fig 2.14a. In this case, the saliency ratio is considered too low, having a value of $L_d/L_q<3$. Fig 2.14b is considered as a single-layer flux-barrier rotor and it is possible to embed permanent magnets in the insulation spacer. This rotor might be a combination of a salient pole and a permanently excited structure. Its saliency ratio can be from 6-8.

Fig 2.14c is an axially laminated rotor, where the highest saliency ratios can be obtained, such as $L_d/L_q >10$ and in the best cases it can reach 15. In the rotor of Fig 2.14d, a cage winding appears as a damper winding in an ordinary salient-pole synchronous machine and the typical values of the saliency ratio in this case is really low, in the range from 3-4.

Another rotor type that may have mounted permanent magnets, if desired, is the one in Fig 2.14e, which is also a single-layer flux-barrier kind. The aim of including the magnets here is to avoid the passing of the flux in the quadrature axis direction. Fig 2.14f represents a multi-layer flux-barrier rotor construction where the quadrature axis reluctance is reduced because of the supports in the round laminates. The maximum possible saliency ratio is 10, in other words, $L_d/L_q < 10$. This rotor type seems to be currently used for commercial versions of SynRMs [11].

Torque production and equation model for a Synchronous Reluctance Motor.

Similarly as the PMSM, the machine characteristics of a SynRM are different in the d and q axes due to the rotor structure; otherwise, the equivalent circuit resembles the one of the IM. In the same manner, there are equivalent circuits analyzing the machine with direct and quadrature reference frame fixed to the rotor:
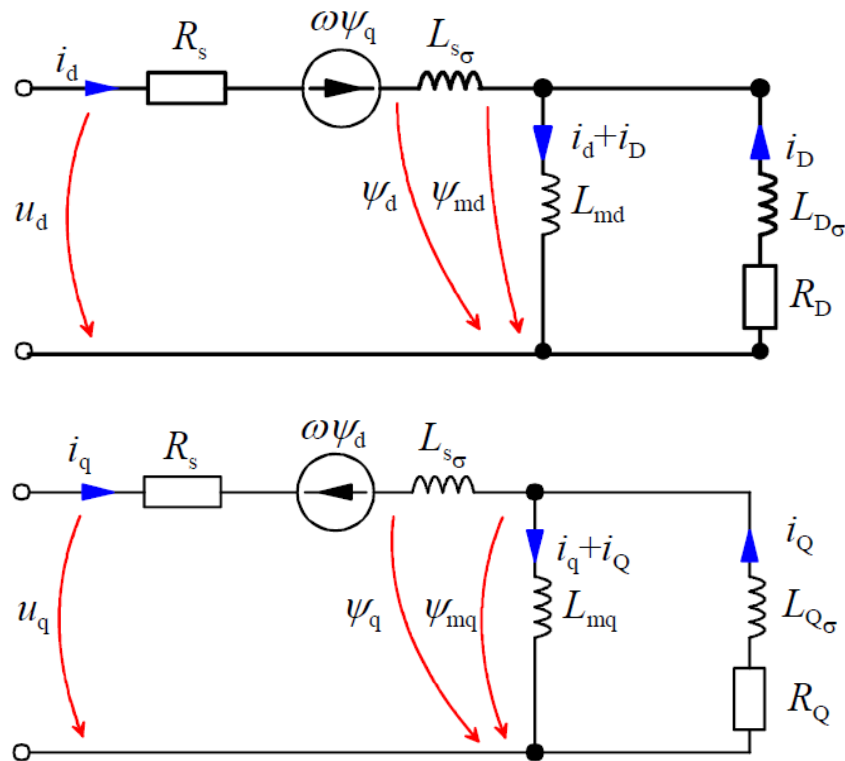
Fig 2.15 Synchronous Reluctance Machine equivalent circuits in d and q directions.

The voltage equations are obtained from those equivalent circuits:

$$u_{sd} = R_s i_{sd} + \frac{d\psi_{sd}}{dt} - \omega\psi_{sq} \tag{2.23}$$

$$u_{sq} = R_s i_{sq} + \frac{d\psi_{sq}}{dt} + \omega\psi_{sd} \tag{2.24}$$

Flux linkage components equations can also be obtained from the circuits:

$$\psi_{sd} = L_{sd} i_{sd} = (L_{md} + L_{s\sigma})i_d + L_{md} i_D \tag{2.25}$$

$$\psi_{sq} = L_{sq} i_{sq} = (L_{mq} + L_{s\sigma})i_q + L_{mq} i_Q \tag{2.26}$$

Stator flux linkage ψ_s of a SynRM contains the stator leakage flux linkage $\psi_{s\sigma}$ and the air gap flux linkage ψ_m:

$$\psi_s = \psi_{s\sigma} + \psi_m \tag{2.27}$$

The stator leakage flux linkage is the product of the stator leakage inductance and the stator current:

$$\psi_{s\sigma} = L_{s\sigma} i_s \tag{2.28}$$

Using the cross field principle, the torque can be shown with the next equation:

$$T_e = \frac{3}{2}p(L_d - L_q)i_d i_q \tag{2.29}$$

Taking into account that the torque-current ratio and the power factor are considered low in a SynRM, different control principles have been developed in order to increase the machine efficiency, based on the two axes model. These control principles require mainly the position of the rotor specifying the rotor angle information. Some typical control methods

are the Current Vector Control, Constant Stator Current Control, Direct Torque Control [17] and Flux Linkage Control, among others [11].

2.2.4 Permanent Magnet-Assisted Synchronous Reluctance Motor

The implementation of permanent magnets is helping the development of synchronous motors with higher efficiency that also reduces power consumption and in consequence, contributes in a certain manner to a global environmental preservation. So far both the PMSM and SynRM have been analyzed and in brief, the first machine type uses a powerful magnetic field flux and the second one uses the reluctance generated by the rotor electromagnetic saliency. SynRM is considered as a low-cost with high efficiency and one of the considerations for this is the fact that it does not have secondary copper losses in the rotor.

Some tests and comparisons have been done in terms of efficiency and the economical point of view between a PMSM with embedded magnets in the rotor (also known as Interior Permanent Magnet Synchronous Motor, IPMSM), a SynRM and an IM, in the same conditions. After the evaluation, the highest efficiency was found in the IPMSM with a value of over 95% but it was not economical due to the costs of the permanent magnets' material. The SynRM gave better results than the IM in both the efficiency and costs [16].

Taking those results into account, the concept of an optimal design that could have a great efficiency at a low cost (meaning a small quantity of magnets) was originated and conceived as a Permanent Magnet-Assisted Synchronous Reluctance Motor (PMASynRM, Fig 2.16) that, compared to a PMSM, can give the same efficiency using only one-fourth the amount of magnets.
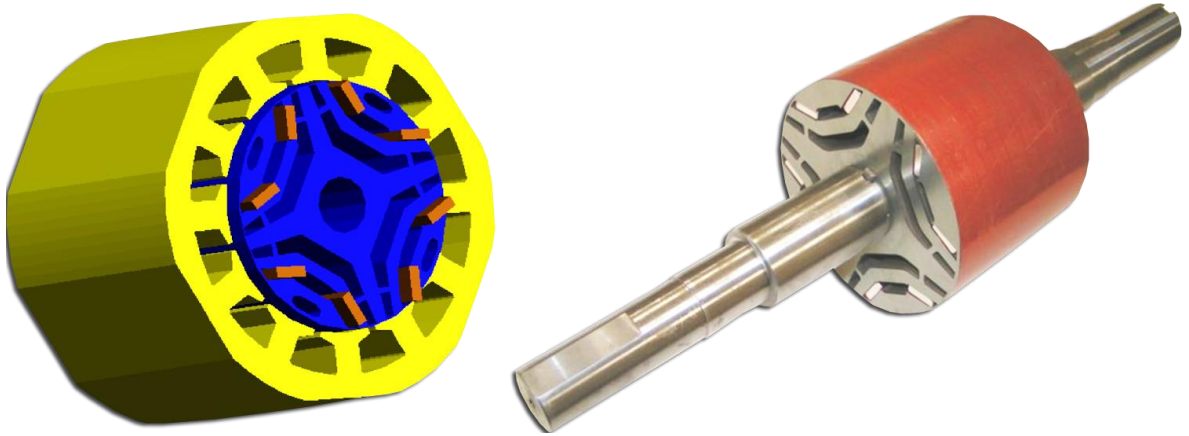
Fig 2.16 PMASynRM rotor construction overview using FEM (left) and a real prototype (right).

Some rotor structures of this so called PMASynRM are shown in Fig 2.17 where (a) and (c) are mostly used for hybrid electric vehicle (HEV) or similar applications. (b), (e) and (f) are examples of the complexity on designs where the insulation layers are really close to the shape of the natural flux lines inside the solid rotor. (d) is a clearer example of the implementation of high quality PM materials such as neodymium (NdFeB) minimizing the volume of the magnet [20].
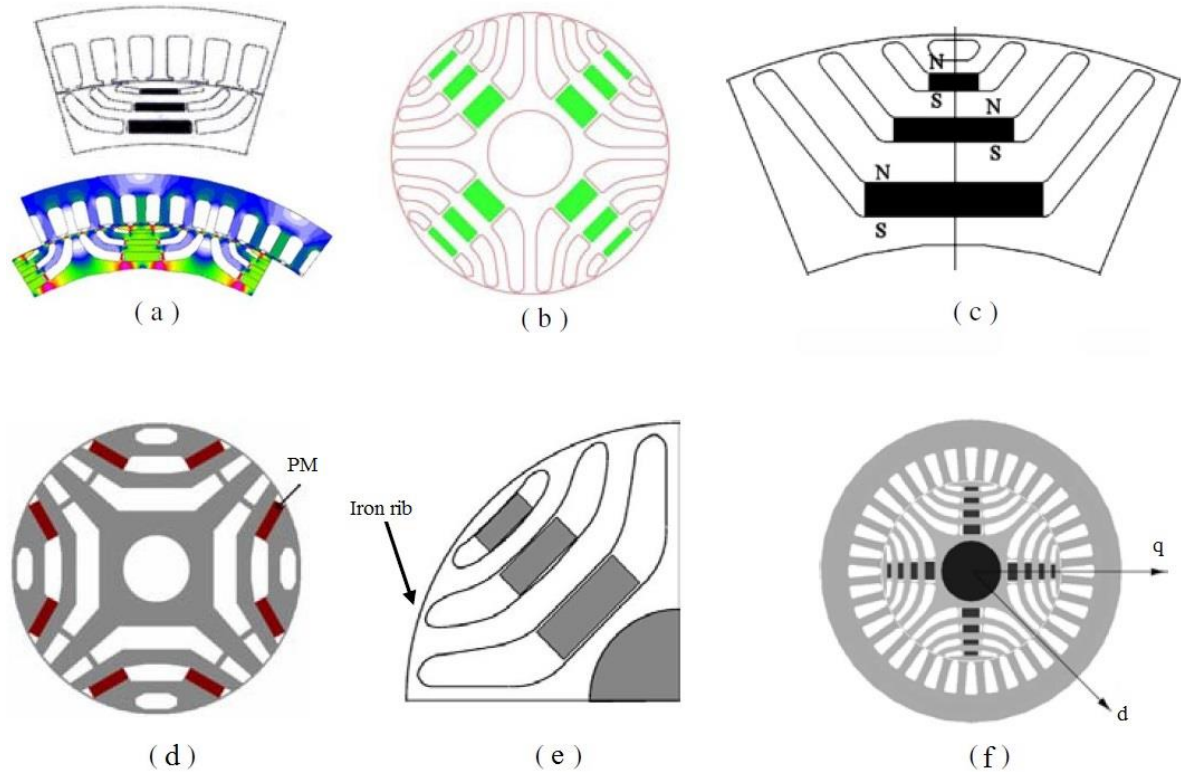
Fig 2.17 Permanent Magnet-Assisted Synchronous Reluctance Machine rotor types.

Torque production and equation model for a Permanent Magnet-Assisted Synchronous Reluctance Motor.

Previously it has been mentioned that the saliency ratio plays an important role in the performance of any SynRM, now considering the addition of the magnets in the rotor, the produced torque will increase whenever the same amount of current is applied, doing it so, the phase voltage should be higher [21].

To obtain the voltage and flux linkage equations, the direct and quadrature axes are the reference frame again and assuming appropriate conditions, the results are the same as equations 2.13 and 2.14 for voltages, equations 2.17 and 2.18 for the flux linkages, all resembling the behavior of the PMSM [22].

The torque equation for the PMASynRM parts from the SynRM (equation 2.29), but the addition of the magnets to the rotor creates a flux linkage that should be included for further analysis [21]:

$$T_{\text{e}} = \frac{3}{2}p\left[(L_{\text{d}} - L_{\text{q}})i_{\text{d}}i_{\text{q}} + \psi_{\text{PM}}i_{\text{sd}}\right]$$

(2.30)

As the name implies, a PMASynRM is a combination of both the synchronous reluctance and the permanent magnet synchronous machines. That fact can be proven with the equations shown so far. The addition of permanent magnets causes an increment in the saliency ratio and in consequence, their difference also increases, leading to the obtainment of a higher power factor and a higher torque [21].

2.3 Comparison including different applications

This section summarizes the arguments for and against within the four types of motors analyzed so far. Different applications have been taken into account to make this comparison and the results are shown in Table 2.1.

Table 2.1 Motor comparison considering different applications.

	IM	PMSM	SynRM	PMASynRM
IM		>IM ease of service is more accessible [23] >IM prices are lower: 1-2 year payback [23] >IM brings more reliability at low production costs [26] >IM provides a wider range of speed [26]	>IM mix and matches motors and drives [23] >IM is available for all kind of applications [23]	>IM torque ripple is higher [27]
PMSM	>PMSM size is smaller [23] >PMSM gives higher power density for its size [25] >PMSMs are more compact, which causes a low rotor inertia and faster response [25] >PMSM noise and vibrations are lower [25]		>PMSM has higher efficiency [16] >PMSM losses (iron, copper) are smaller [16] >PMSM power factor is higher [16]	>PMSM power factor is higher [16]
SynRM	>SynRM has better efficiency [16] >SynRM costs are lower [16] >SynRM has no slip frequency between the stator and the rotor [24] >SynRM size is smaller [23] >SynRM has pre-selected motor-drive packages [23]	>SynRM is cheaper because PMSM uses a large amount of expensive magnets [16]		>SynRM is easier to manufacture [23]
PMASynRM	>PMASynRM rated torque is higher [27] >PMASynRM has higher output power [27] >PMASynRM efficiency and power factor are bigger [27] >PMASynRM total weight is lighter [27]	>PMASynRM has larger saliency ratio [22] >PMASynRM reluctance torque is more important [22] >PMASynRM can give the same efficiency with one-fourth the amount of magnets [16]	>PMASynRM d-q inductances difference is bigger [21] >PMASynRM power factor is higher [21] >PMASynRM has larger torque density of the motor [21] >PMASynRM losses are smaller [16]	

The numbers inside brackets correspond to the reference of the documents at the bottom of this paper. In the list below, the content of each reference is named according to its application.

[16]   Performance evaluation made out of four different rotor types.

[21]   Effects of rotor structure on torque by means of Finite Element Method (FEM).

[22]   Air-conditioner compressor.

[23]   Innovative motor and drive package.

[24]   Online parameter identification for sensorless control.

[25]   Cooling towers.

[26]   Hybrid electrical vehicles.

[27]   Electric motor for existing vessels and future ships and submarines.

2.4 High efficiency pump motors

The International Electrotechnical Commission (IEC) published the standard IEC 60034-30-1 in March 2014 related to the energy efficiency classes for electric motors, covering a wide range that goes from 0.12 kW to 1000 kW, single and three phase motors, both 50 and 60 Hz frequencies and the number of poles 2, 4, 6 or 8. It is important to notice that this standard does not cover motors completely integrated into a machine [28].

The efficiency classes defined by IEC 60034-30-1 are:

- IE1 Standard efficiency
- IE2 High efficiency
- IE3 Premium efficiency
- IE4 Super-Premium efficiency

An example of the classification can be seen in Fig 2.18 that shows different output values and their minimum efficiencies.
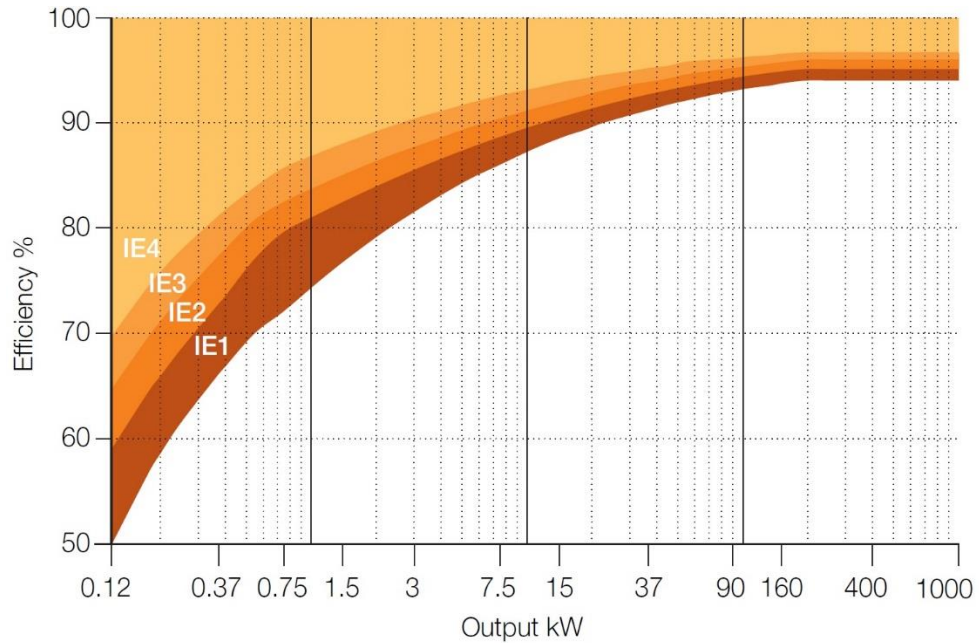
Fig 2.18 IE efficiency classes for 4 pole motors at 50 Hz

Apart from these four classes, a new level named IE5 is expected to emerge in future revisions. The aim of IE5 will be to reduce losses by 20% compared to the IE4 class [28].

Since January 2015, motors from 7.5 kW to 375 kW must reach the IE3 efficiency level, or at least they should include a VSD to meet the requirements imposed by the IEC. By January 2017 these regulations will be extended down to motors of 0.75 kW [29].

ABB introduced a magnet free IE4 SynRM back in 2011, it was a big achievement because this efficiency level was established three years later. Demands for increasing the efficiency force an Original Equipment Manufacturer (OEM) to find new solutions in order to reduce the energy consumption and ABB is no exception, as a reply for this demand, the company is introducing the new SynRM^2 technology which claims to reduce motor losses by 20%, achieving the IE5 Ultra-Premium efficiency [30].

The SynRM^2 technology platform (Fig 2.19) contains ferrite magnets, which are especially more cost effective and also easier to source than the rare earth magnets. As a result, the motor is more sustainable in both aspects economic and ecological. The mentioned technology is quite flexible since it is optimized to meet the technical and commercial characteristics according to the customer requirements.

Fig 2.19 SynRM2 technology concept.

Another example of high efficiency pump motors is the speed-controlled KSB SuPremE (Fig 2.20) with a wide variety of applications. This SynRM already meets the IE4

efficiency requirements and even exceeds the regulations of the European ErP (Energy related Products) for 2017. It is built without magnetic materials and in hence the total environmental footprint is smaller than in the case of PMSMs. The rating power can be from 0.55 to 45 kW [31].
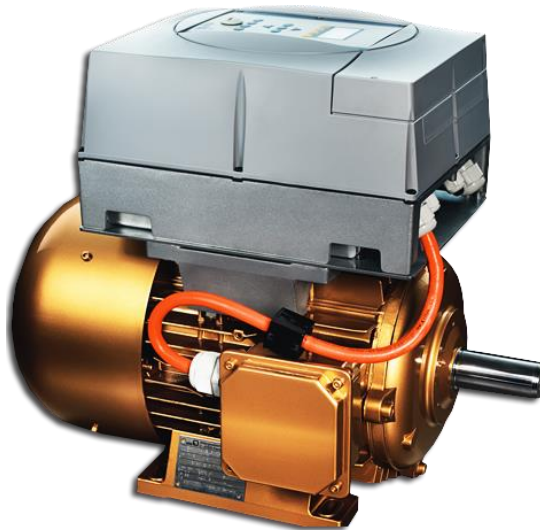
Fig 2.20 KSB SuPremE high efficiency SynRM.

Chapter 3

3 Evaluation of 15 kW motors

3.1 Motor characteristics comparison

From this stage of the study, we will be focusing in the 15 kW motors to evaluate, at first instance, an induction motor and a SynRM since they are in the facilities of the LUT laboratories, allowing us to run certain tests to obtain some electrical parameters and the most important part of this paper: efficiency results, from where we can trace and create graphics and also efficiency maps. Afterwards, some other comparisons will be made including results from simulations of a PMSM using Finite Element Methods (FEM) to extend the motor efficiency comparison study.

In the first place, the motor nameplates from the IM and SynRM located in the LUT laboratories will be shown and explained in Fig 3.1, according to their respective product codes to have an overview of the characteristics of both motors.
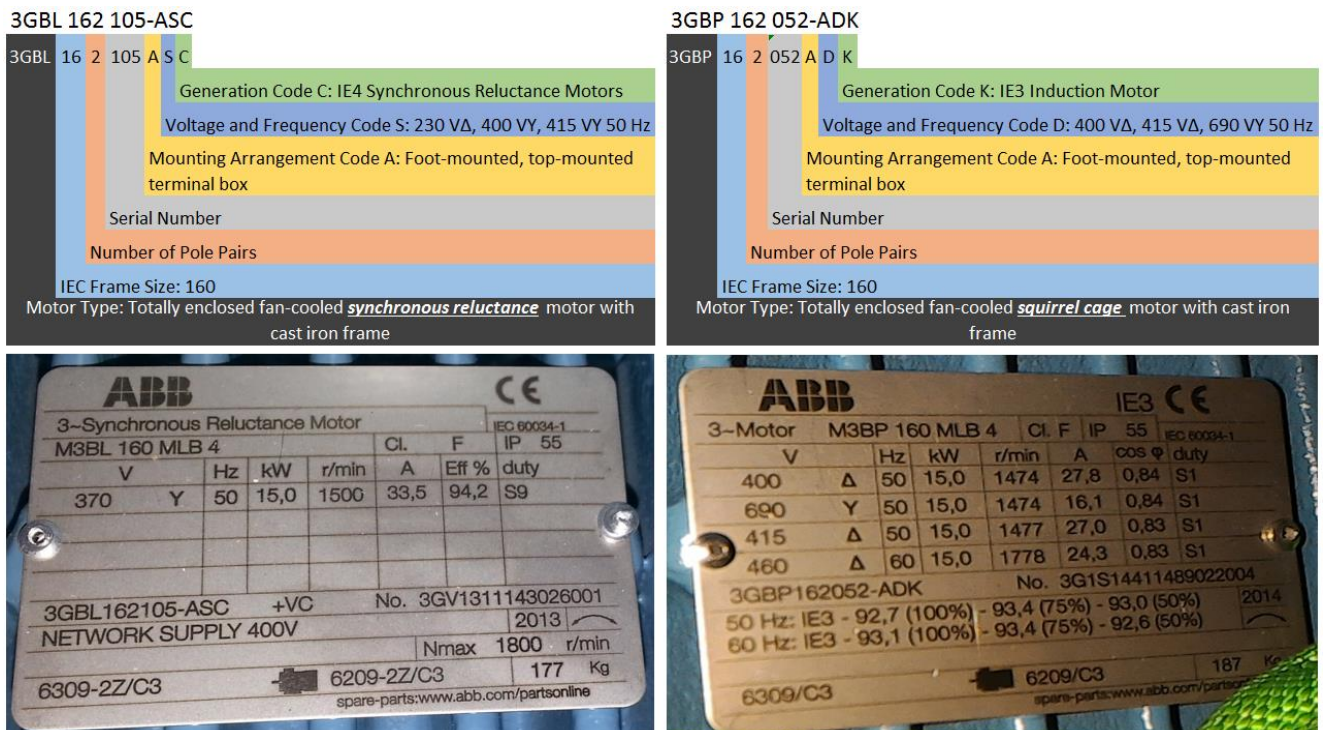
Fig 3.1 Nameplates explanation for the IM and SynRM in LUT laboratories.

Secondly, the similarities between the two mentioned types of motors, in terms of construction, dimensions and other characteristics will be shown in **Table 3.1**.

Table 3.1 Dimensions and other characteristics for the IM and SynRM in LUT laboratories.

	IM (3-phase)	SynRM (3-phase)
Mounting	IM1001, B3 (foot)	IM1001, B3 (foot)
Type of duty	S1(IEC) 100%	S1(IEC) 100%
Nominal torque T_N	97Nm	95Nm
Insulation class / Temp. class	F / B	F / B
Ambient temperature	40°C	40°C
Altitude	1000 m.a.s.l.	1000 m.a.s.l.
Enclosure	IP55	IP55
Cooling system	IC411 self-ventilated	IC411 self-ventilated
Bearing DE/NDE	6309/C3 - 6209/C3	63092Z/C3 - 62092Z/C3
Position of terminal box	Top	Top
Total weight of motor	187Kg	177Kg
Number of poles	4	4
Product IE Class	IE3	IE4
Frame material	Cast Iron	Cast Iron
Length	681mm	671.5mm
Width	338mm	338mm
Height	421mm	421mm
Price (VAT 0%)	1 810 €	2 014 €
ACS850 Price (VAT 0%)	1 050 €	

The type of mounting is the same for both motors (IM1001 B3), it is foot-mounted with the terminal box on top, the type of duty is also the same (S1), considered as a continuous duty where the motor keeps working at a constant load long enough to reach the temperature equilibrium, the nominal torque varies only for 2Nm, the insulation class F and temperature class B mean in brief that the safety margin goes up to 25°C, both motors may work at a maximum ambient temperature of 40°C and at an altitude of 1000 meters above sea level.

The type of enclosure is the same (IP55) and means that it is dust-protected and also with protection against water jets, the same cooling system is used in both motors (IC411) so that the frame surface uses a primary and a secondary coolant with self-circulation. The type of bearings is also the same used in both motors, named as "deep groove ball bearings", but for the SynRM they are shielded to prevent incoming dirt, that is defined by the 2Z ending in the bearing part number.

The total weight of the motor is quite similar, just about 5% heavier in case of the IM. About the physical dimensions they only vary by the length a bit, being the SynRM larger than the IM.

There are other characteristics where we can compare the motor types, but it will lead to an extensive study which cannot be covered on this thesis. For example, the type of bearings has a slight difference as it was just mentioned and along with other components or materials, there may be small mechanical losses to consider for comparison. That is why we are focusing on the most relevant characteristics of the motors.

3.2 Motor efficiency comparison

Several tests were performed inside the LUT laboratories (Fig 3.2), setting parameters such as speed, frequency, current, voltage, references according to nominal values, etc. that led to the obtainment of efficiency measurements and other results for both the induction motor and the SynRM when driven by a VSD. It is important to mention that those tests took place while using constant flux.

Fig 3.2 Motor settings for test in LUT laboratories.

As a result, we were able to compare also the efficiency measurements against the manufacturer's declaration in the motor data sheet, considering six different speeds, starting with 750 rpm and finalizing with the nominal speed value of 1500 rpm. There was also the need of interpolate the data to construct new points for each curve within the range of the already known data points as seen in Fig 3.3 in order to obtain the efficiency curves.
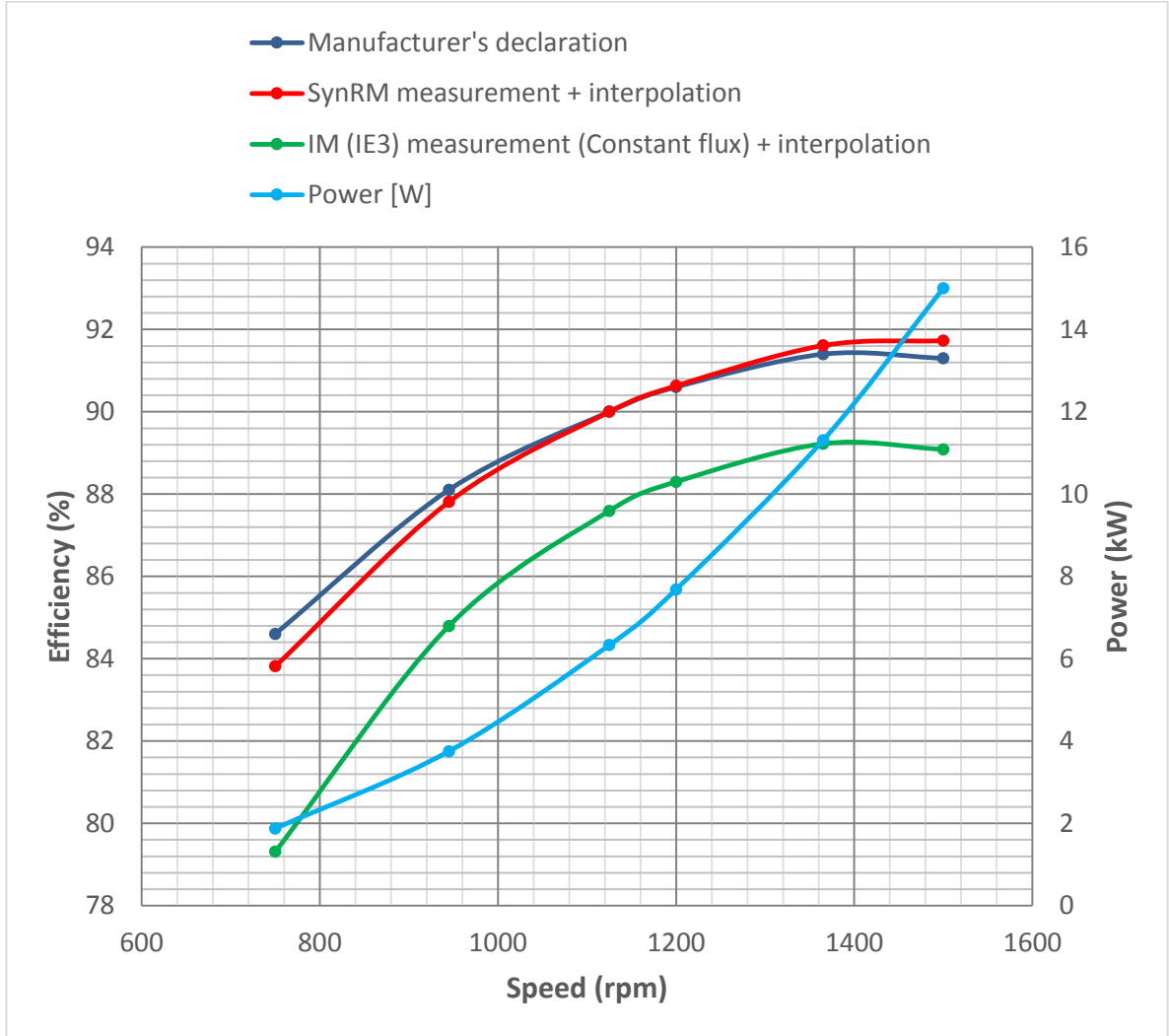
Fig 3.3 IM and SynRM efficiency comparison.

We can see from the figure above that the efficiency curve declared by the manufacturer in the case of the SynRM (dark blue) looks quite similar to the curve of the motor measurements inside the laboratory (red), it is even showing a higher efficiency percentage at 1500 rpm in the red curve, reaching 91.73% compared to the stated 91.3% from the manufacturer, meaning that the tests were successful and accurate considering all of the parameters used. That small difference is also justified taking into account the tolerances for rotating electrical machines defined by the standards IEC 600 34-1 and IEC 600 34-2 [35].

In addition, we can appreciate the efficiency curve of the induction motor (green) and notice the difference from the IE3 (IM) to the IE4 (SynRM) classes, being continuously higher at about 2% from 1125 rpm to 1500 rpm in favor of the synchronous reluctance motor (red). It is also shown the power consumption curve (cyan) at the different speeds, where the starting point is located at 1.8 kW in 750 rpm and the last one at 15 kW in nominal speed of 1500 rpm.

Another test was performed using the same Variable Speed Drive for both IM and SynRM motors. In this case, the selected VSD model was ACS850-04 [32] which is suitable for the frame size of the motors and also because the electrical and mechanical installation in the laboratory facilities were optimal for the equipment. It is important to mention that the IM was operated at constant flux according to standard instructions. This VSD is an air-cooled module and it is also capable of controlling permanent magnet motors.

Apart from the drive efficiency, load points were considered for the mechanical torque (as a percentage of the nominal torque) along with the different speeds for both motors, resulting in the next detailed figure:
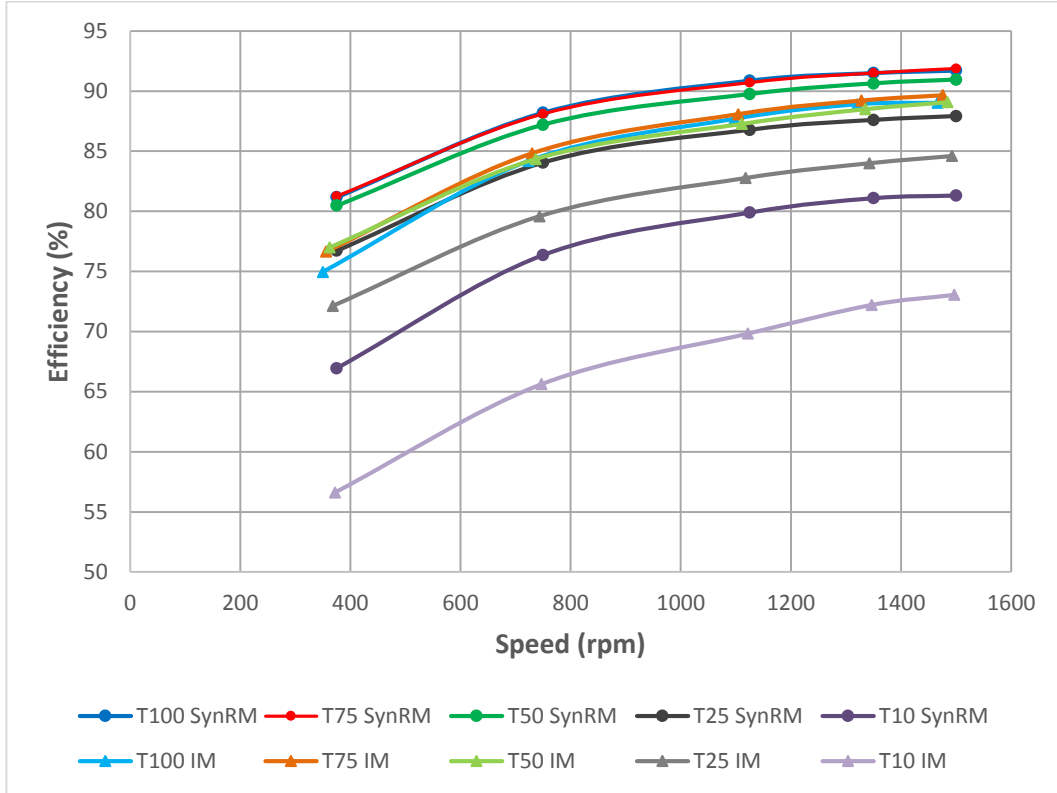
Fig 3.4 Efficiency VS Speed curves at different torque load points.

For instance, "T75 SynRM" (orange) indicates the curve taken at 75% torque in different speeds for the synchronous reluctance motor and "T25 IM" (cyan) is the curve at 25% torque in different speeds for the induction motor. We can see that at 75% of the mechanical torque, the higher efficiency is being reached in both motors while operating at the highest speed of 1500 rpm, in fact, this applies to all of the different speeds in the exclusive case of the IM.

From T50 to T100 and comparing IM VS SynRM, the difference in efficiency terms is about 5% in all cases, but from T10 to T25 is much bigger, this is due to the constant flux control where the magnetizing current is kept constant and all of the reactances vary whenever the frequency is changing in an IM [36], that is why a SynRM is more suitable for pumping applications.

3.3 Pumping system requirements

Pumping systems can be categorized in two different types: closed and open systems. In the closed systems, the heat energy is transported into the heating or air conditioning systems, cooling systems, etc. where the liquid itself circulates and is the carrier of the heat energy. In open systems, the pump transports the liquid from point to point like in an irrigation system or water supply system. We can see an example of how these two pumping systems operate in a very basic way on figures Fig 3.5a and 3.5b.
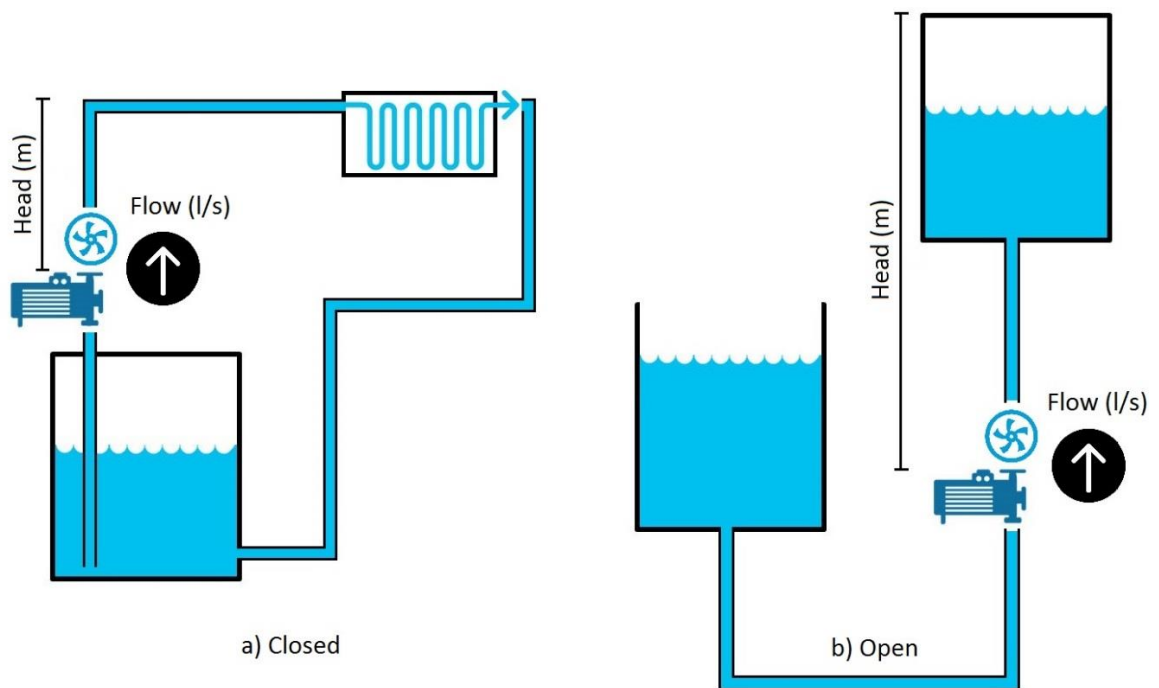
Fig 3.5 a) Closed loop system b) Open loop system.

Pump performance is one of the key concepts that are being considered on this study, for that reason, it is important to define two basic terms that will help us to understand further analyses: the flow (Q) and the head (H). Flow means the amount of liquid going through a pump during a determined period of time, usually expressed in liters per second (l/s). Head indicates the altitude that a liquid can be lifted by the pump, expressed in meters (m).

Pump performance curves (Fig 3.6) help to define how efficiently the pump will operate in terms of head and flow, showing the possible operating conditions. The diameter of the impeller installed in the pump casing is also an important factor since a larger diameter allowed gives the best efficiency because less fluid is slipping between the impeller blades and the pump casing. As an example, the impeller diameters are shown in the figure below, with values of 272, 250, 225 and 200 millimeters.
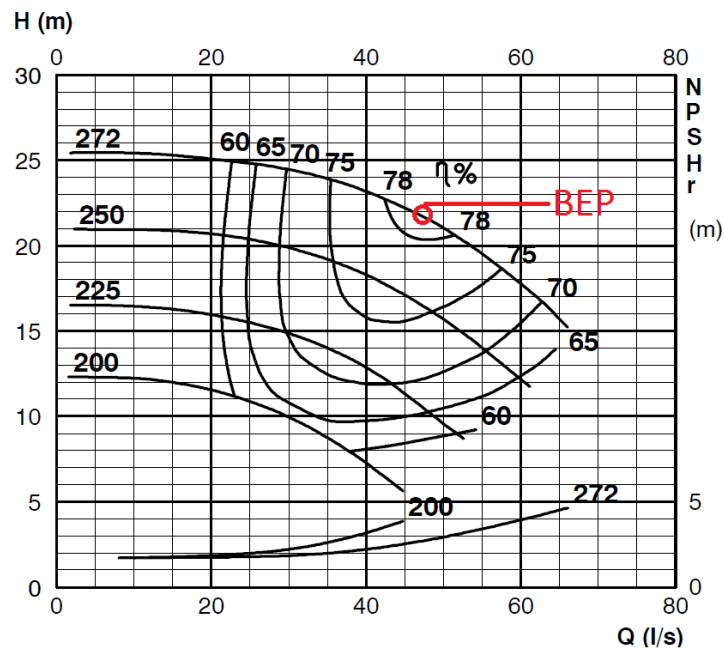
Fig 3.6 Pump performance curves (also known as characteristic curves).

The actual pump efficiency (η) is also shown as percentages in the same graphic, crossing with the head curve and it represents or gives the idea of the best efficiency point (BEP) where the pump may operate. Other points located at the left or right of the BEP indicates a lower efficiency. Total efficiency will never be reached since there are mechanical and hydraulic losses in the pump, that is why the pump must be selected closer to the BEP, to guarantee the highest possible efficiency and not only that, also to improve the life time and reliability of the pump [33].

Fig 3.6 is the specific case for the Sulzer APP-31-100 centrifugal pump in a closed loop system, this will be part of the case of study in the coming sections, since some other tests and simulations were performed with this pump in order to obtain results of the efficiency at different speeds, and also to obtain the torque at different load points.

Before going into details of those results, it is important to understand how the variation of speed affects the flow rate, head and power and in hence, the performance of the pump. In order to do it, we will consider the Affinity Laws for pumps which will lead to calculate the performance changes depending on the speed.

There are 3 affinity laws related to the rotational speed (n), which indicates that:

1) The flow rate (Q) is proportional to the speed.

$$\frac{Q_1}{Q_2} = \frac{n_1}{n_2} \tag{3.1}$$

2) The head (H) is proportional to the square of speed.

$$\frac{H_1}{H_2} = \left(\frac{n_1}{n_2}\right)^2 \tag{3.2}$$

3) The power (P) is proportional to the cube of speed.

$$\frac{P_1}{P_2} = \left(\frac{n_1}{n_2}\right)^3 \tag{3.3}$$

The equations above indicates that, if you double the speed, the flow will also double, the head increases by four and the power increases by eight. In an opposite point of view, reducing the speed leads to a very large reduction in power consumption. This is one key point of the study since we will be able to solve the needed speeds for a lower energy consumption. Controlling the flow using valves does not effectively reduce the power

consumption, which is why speed regulation is highly recommended, it also reduces vibration and noise and the bearings lifetime is extended [34].

Applying the affinity laws from equations 3.1 and 3.2 and according to the load profile for a closed loop system [37], we were able to solve the needed speeds for the Sulzer centrifugal pump (Fig 3.7), following the performance curve from the nominal speed and now converted to different speeds:
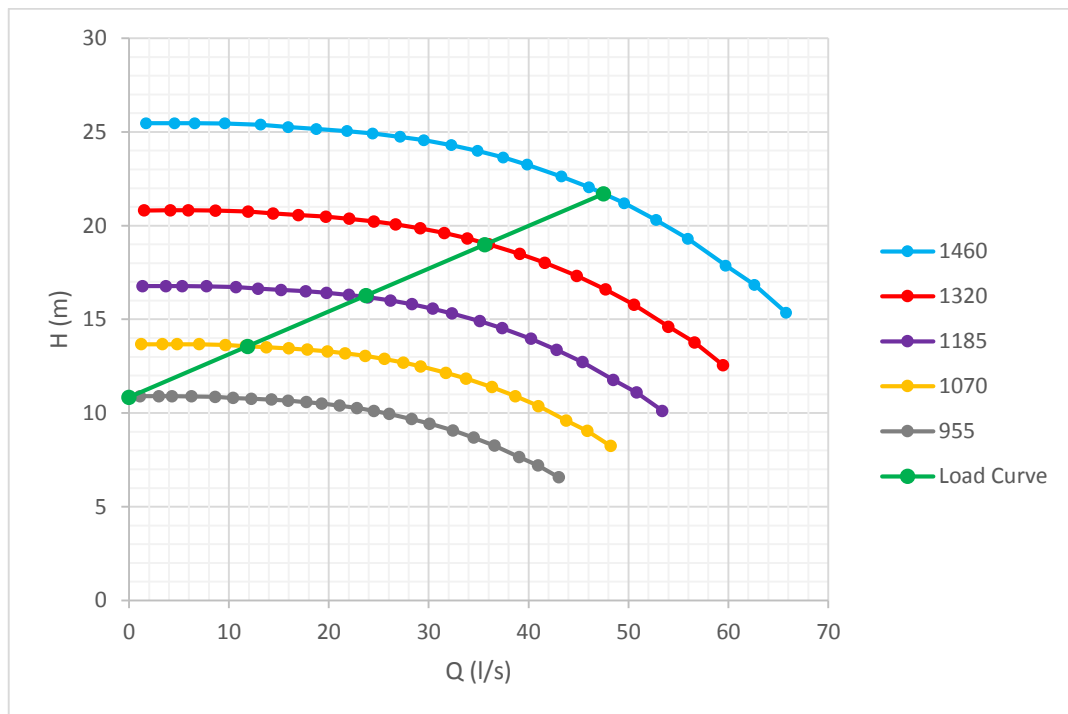
Fig 3.7 Needed speeds using affinity laws.

The nominal values for this pump are: Head = 21.7m, Flow = 47.5 l/s, Speed = 1460 rpm and Power = 12.9 kW. The load curve (green) is then drawn at 0-25-50-75-100 % Flow, where the maximum one crosses the 1460 rpm curve at the actual location of the BEP. We can see other speeds also to verify where their BEPs would be located at certain flow rate.

In a similar way, but now using affinity laws equations 3.1 and 3.3 and having the already solved speeds, we are able to draw the curves to obtain the power consumption also according to the required flow rate at the given speeds.
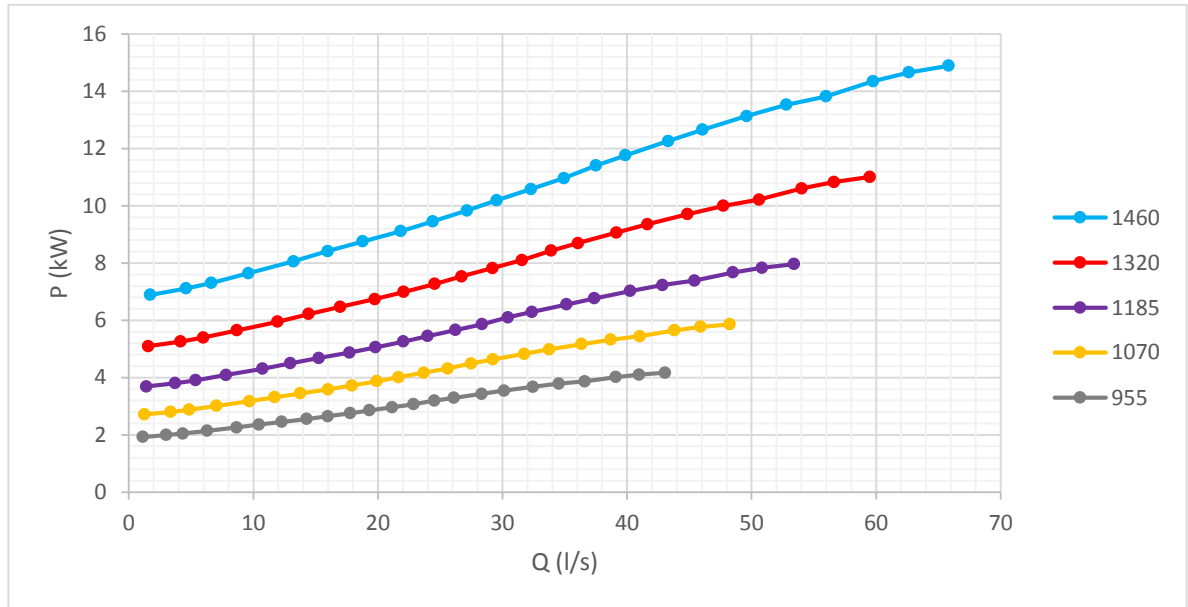
Fig 3.8 Power consumption at solved speeds using affinity laws.

We can notice that at 100% flow (47.5 l/s) for 1460 rpm, the power consumption reaches 12.8 kW and for example, at 50% flow (23.75 l/s) of the 1185 rpm speed the power consumption is about 5.4 kW. Having these values of power and speed, it is possible to calculate the load torque needed for running the Sulzer pump and finally trace efficiency maps, which will be very helpful to compare the motor types.

A simple formula of the torque related to power and speed will be used in order to obtain the points of measurements and it is defined in the next equation:

$$T = \frac{P}{\omega} \tag{3.4}$$

where T is the torque in Nm, P is the power in watts and ω is the angular speed computed with the formula:

$$\omega = \frac{2*\pi*rpm}{60}$$ (3.5)

rpm is the given speed, in our case, the different speeds that have been solved so far.

The most relevant results obtained so far are summarized in **Table 3.2**, expressed also as a percentage of the SynRM nominal values.

Table 3.2 SynRM performance with the Sulzer pump.

Flow (l/s)	Speed (rpm)	Power (kW)	Torque (Nm)
47.5 (100%)	1460 (97.3%)	12.8 (85.4%)	83.7 (88.1%)
35.62 (75%)	1320 (88%)	8.6 (57.5%)	62.4 (65.7%)
23.75 (50%)	1185 (79%)	5.4 (36.2%)	43.8 (46.1%)
11.87 (25%)	1070 (71.3%)	3.3 (22.1%)	29.6 (31.2%)

We can see clearly the advantage of using a motor driven by a VSD, for instance, to obtain the maximum flow, we require 97.3% of the motor's nominal speed, but in terms of power, the energy consumption savings are noticeable, since it requires only 85% of the nominal power. At half flow of the pump, the needed speed is around 80% of the nominal value and the power consumption is now 36% when in the case of valve control the power consumption would be around 9.3 kW (62%). In a similar way we can compare the shaft torque requirements as a percentage of the nominal value, which is 95 Nm in the case of this SynRM.

3.3.1 Efficiency of 15 kW SynRM drive

Based on the manufacturer's statement for the case of the SynRM, the efficiency map was then calculated, showing the motor speed vs load torque and the efficiency of the motor at different points, which can be seen in the figure below:
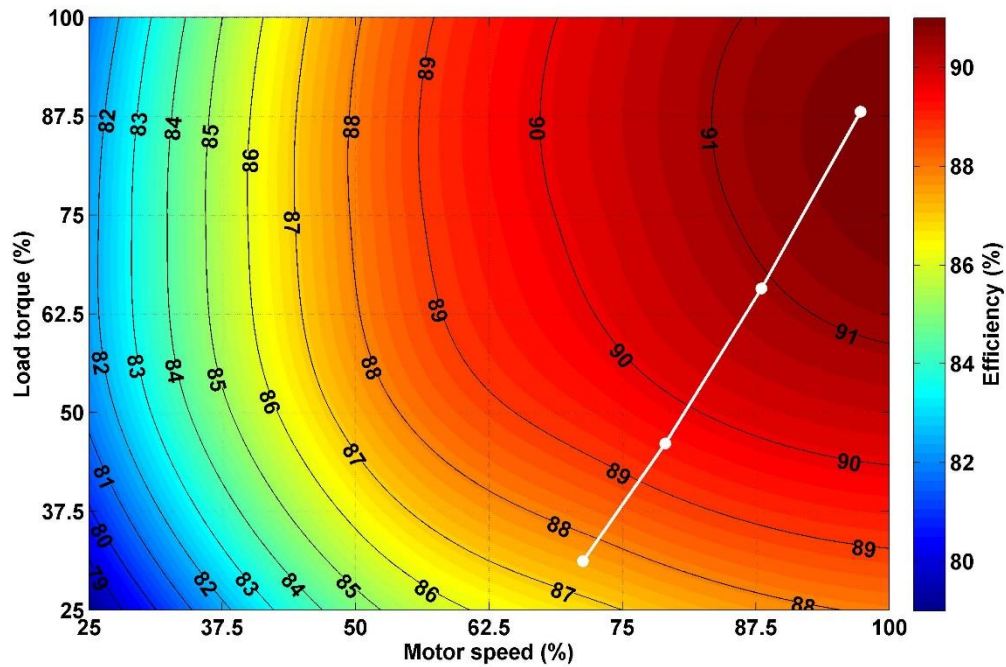
Fig 3.9 Efficiency map for the SynRM.

Black curves and color map in Fig 3.9 are representing the SynRM package efficiency. In addition, the white dots indicate the needed torque for running the Sulzer pump with the SynRM, also known as the operating points in this case using the load profile for closed loop systems [38]. At 97% speed, the pump only requires about 88% of the motor nominal torque which means a lower energy consumption, so instead of using the full power of the motor (15 kW), the pump only requires less than 13 kW to give the nominal flow of 47.5 l/s and head of 21.7m.

We can see the efficiency values and needed speed and torque corresponding to the operating points from Fig 3.9 shown in the table below.

Table 3.3 Operating points for the pump driven with a SynRM.

Speed (%)	Torque (%)	Efficiency (%)	Input Power (kW)
97.3	88.1	91.3	12.8
88	65.7	90.9	8.62
79	46.1	89.4	5.43
71.3	31.2	87.5	3.32

3.3.2   Efficiency of induction motor drive

In a similar way and using the results from the tests running inside LUT Laboratories, the efficiency map for the induction motor was also obtained and it is shown in Fig 3.10.
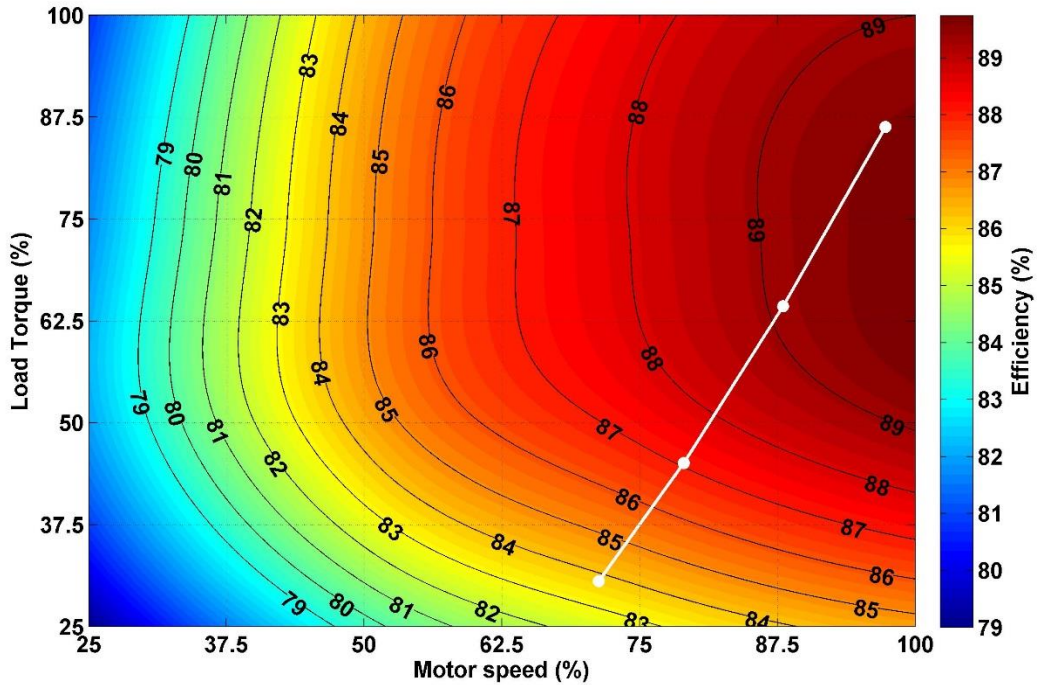
Fig 3.10 Efficiency map for the IM.

It is important to mention that the operating points are being considered at the same speed values since we are evaluating one pump only, so they are distributed in the same location of the x axis in both figures Fig 3.9 and Fig 3.10, the efficiency map is indeed different and we can see that for the IM, the two highest operating points remain above the 89% line. Comparing the previous two figures, we can notice the advantage in terms of efficiency when using the SynRM over IM. The operating point values of the IM can be seen in the next table.

Table 3.4 Operating points for the pump driven with an IM.

Speed (%)	Torque (%)	Efficiency (%)	Input Power (kW)
97.3	86.3	89.3	12.79
88	64.3	89.1	8.62
79	45.1	87.3	5.42
71.3	30.6	83.9	3.32

3.3.3 Effect of dimensioning on the SynRM efficiency

Now if we try the over dimensioning of the SynRM in order to have an idea on how the size of the motor and characteristics such as power, torque, etc. will compare to our current 15 kW motor, we can also obtain the efficiency map. So we are considering only commercially available values and the closest one above is a motor with 18.5 kW input power and 118 Nm torque. Results are shown in the figure below:
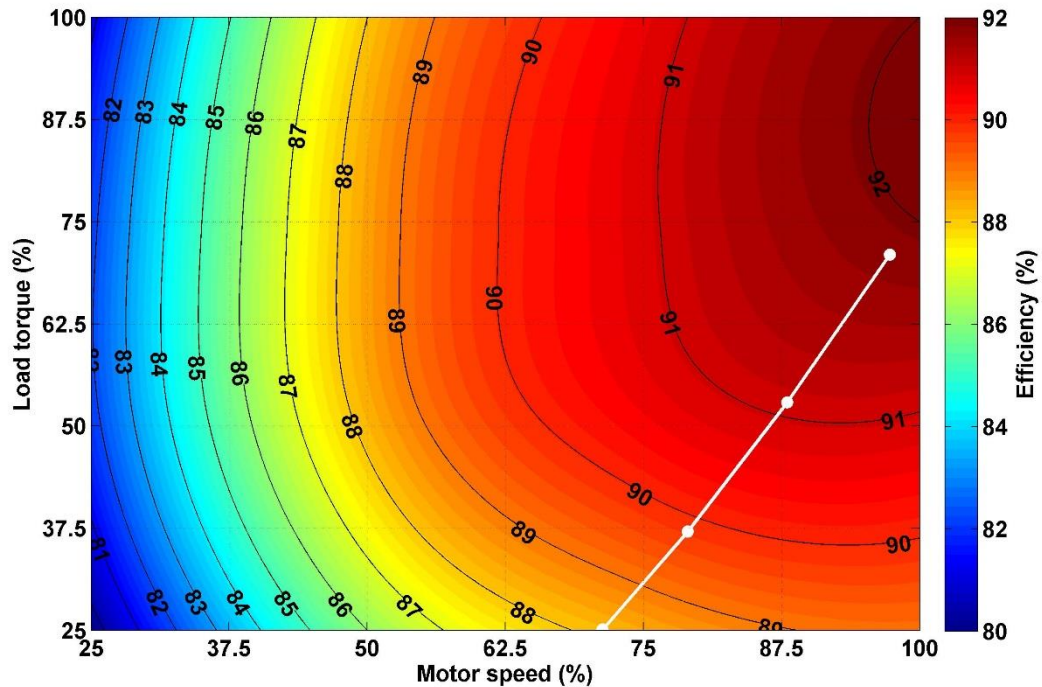
Fig 3.11 Over dimensioning of the 15 kW motor with an 18.5 kW SynRM.

The operating points now correspond to the 18.5 kW motor and the more noticeable thing to mention is that the torque used even at the maximum efficiency point is just above 70% and the efficiency itself is close to the 92% curve, this could mean some advantages to be reflected into energy savings even if the difference between these motors is 3.5 kW only. On the other hand, if a smaller motor would be used instead of 15 kW motor, for instance

the next value commercially available would be 11 kW but the torque requirements go up to 120% in order to fulfill the desired operating points' efficiency.

The speed, torque, efficiency and input power of the 18.5 kW SynRM package are shown below, according to the efficiency map from Fig 3.11:

Table 3.5 Operating points for the pump driven with the over dimensioned SynRM.

Speed (%)	Torque (%)	Efficiency (%)	Input Power (kW)
97.3	70.9	91.7	12.68
88	52.8	91.1	8.54
79	37.1	89.8	5.38
71.3	25.1	88.2	3.29

3.4 Results for 15 kW motors

With the results obtained so far, mainly the power consumption of the pump and the package efficiency, we can determine the energy consumption values using the time distribution for closed loop systems given in the table below:

Table 3.6 Time distribution for closed loop systems.

Flow (%)	Time (%)
100	6
75	15
50	35
25	44

These values bring the idea on how the pump behaves in the closed loop systems, where it usually is running only a small fraction of time on full flow and on the other side, most of

the time the pump is running on a low flow rate, which highlights the importance of using a VSD so that the flow can be controlled at a certain speed to save energy.

In this study, we will consider the pump running a total of 4160 hours per year (47%) with a calculated average power consumption of 6.06 kW, using the time distribution from Table 3.6 for the SynRM and information from Table 3.3, this brings a total of 25,222 kWh as a total energy consumption through one year. In comparison with a fixed speed motor of the same characteristics, the benefits of the SynRM are close to 13% less energy consumption.

With the same amount of hours per year, but with the average power for the IM with a VSD calculated as 6.23 kW based on Table 3.4, the energy consumption in one year would be 25,933 kWh. Values for the PMSM were also estimated and a complete table showing all of them will be used for comparison, based on the same time distribution and including the energy costs per year considering the electricity price as 0.07 € per kWh:

Table 3.7 Energy consumption and costs for different motors.

Motor type	Average power (kW)	Consumption in 1 year (kWh)	Energy costs in 1 year (€)
SynRM	6.06	25,222	1,765.55
IM with VSD	6.23	25,933	1,815.34
IM fixed	6.86	28,545	1,998.21
PMSM	5.81	24,173	1,692.16

3.5 Potential of higher efficiency motors in the closed-loop application

So far we have seen comparisons between IE3 and IE4 motor classes. In a similar way than Fig 2.18, more efficiency classes can be shown in the same graphic even if they are not commercially available yet. That is the case of the 2nd edition of the IEC 60034-30 standard

which includes now the IE5 class and establishes the current efficiency limit study (Fig 3.12), which may vary throughout the coming ten years for instance and even a higher efficiency class IE6 may appear in the graphic whenever new technologies may rise concerning the improvement of the motor efficiency.

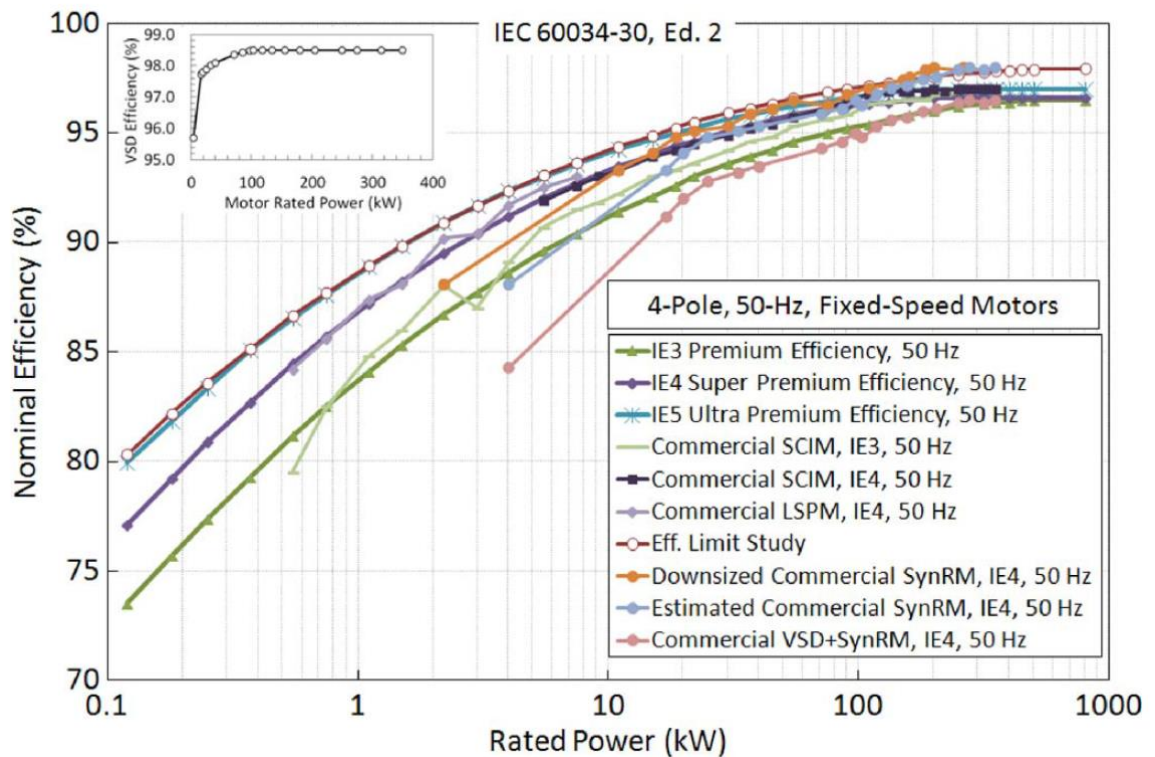Fig 3.12 Efficiency classes according to the 2nd edition of the IEC 60034-30 standard [39].

With that IE5 Ultra Premium Efficiency in mind and using FEM to simulate a PMSM with similar characteristics as the previous IM and SynRM studied motors, we were able to obtain the efficiency map for the permanent magnet motor, where the effect of the VSD and some mechanical losses are also contemplated:
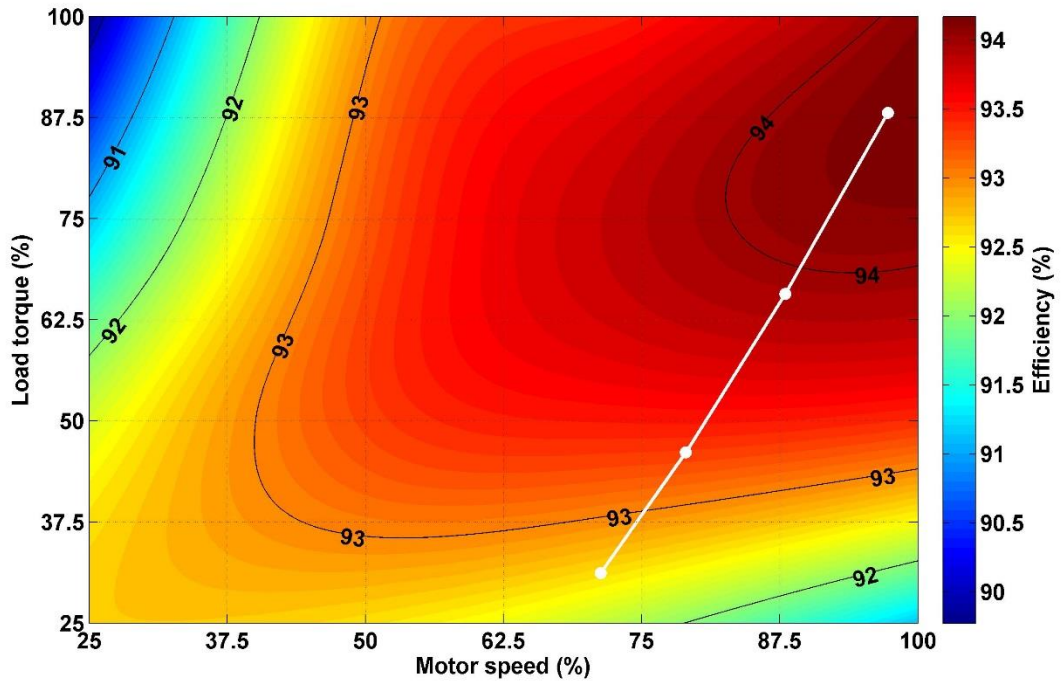
Fig 3.13 Efficiency map for the PMSM.

Comparing the previous efficiency map with Fig 3.12, we can notice that this designed PMSM fulfills the requirements for the IE5 class, where the 15 kW motor reaches almost 95% efficiency at its maximum peak. The operating points for the pump that has been part of the study are also present on this efficiency map, where the majority of points are located near and above the 93% efficiency line, this will of course be reflected as energy savings since the pump will be running with an IE5 motor.

Table 3.8 Operating points for the pump driven with the designed PMSM.

Speed (%)	Torque (%)	Efficiency (%)	Input Power (kW)
97.3	88.1	94.5	12.79
88	65.7	93.8	8.63
79	46.1	93.3	5.43
71.3	31.2	92.5	3.32

Chapter 4

4 Comparison of resulting energy costs between the studied cases

On the economical side and according to Table 3.7, the energy costs during one year while running the pump with the SynRM are about 1765 € and for a fixed speed motor it would be almost 2000 €, of course the investment costs for the SynRM are higher because it requires a separate VSD unit to operate, which is not needed for a fixed speed motor, but in a longer term the benefits of using the motor and VSD together will translate into energy cost savings and in this particular case of our study, even the CO_2 savings can be estimated with a value close to 3 tons during one year.

From Table 3.7 we can also conclude that the energy consumption compared to the IM while running a VSD will be about 97% for the SynRM and close to 94% in the case of the PMSM, hence this proves the difference between the efficiency classes IE3 (IM), IE4 (SynRM) and IE5 (PMSM).

In the coming figure we are doing a comparison on how these classes will compare with each other in terms of the investment costs and through their annual energy consumption to indicate at what stage a class payback time comes out and makes that class more profitable than the other.
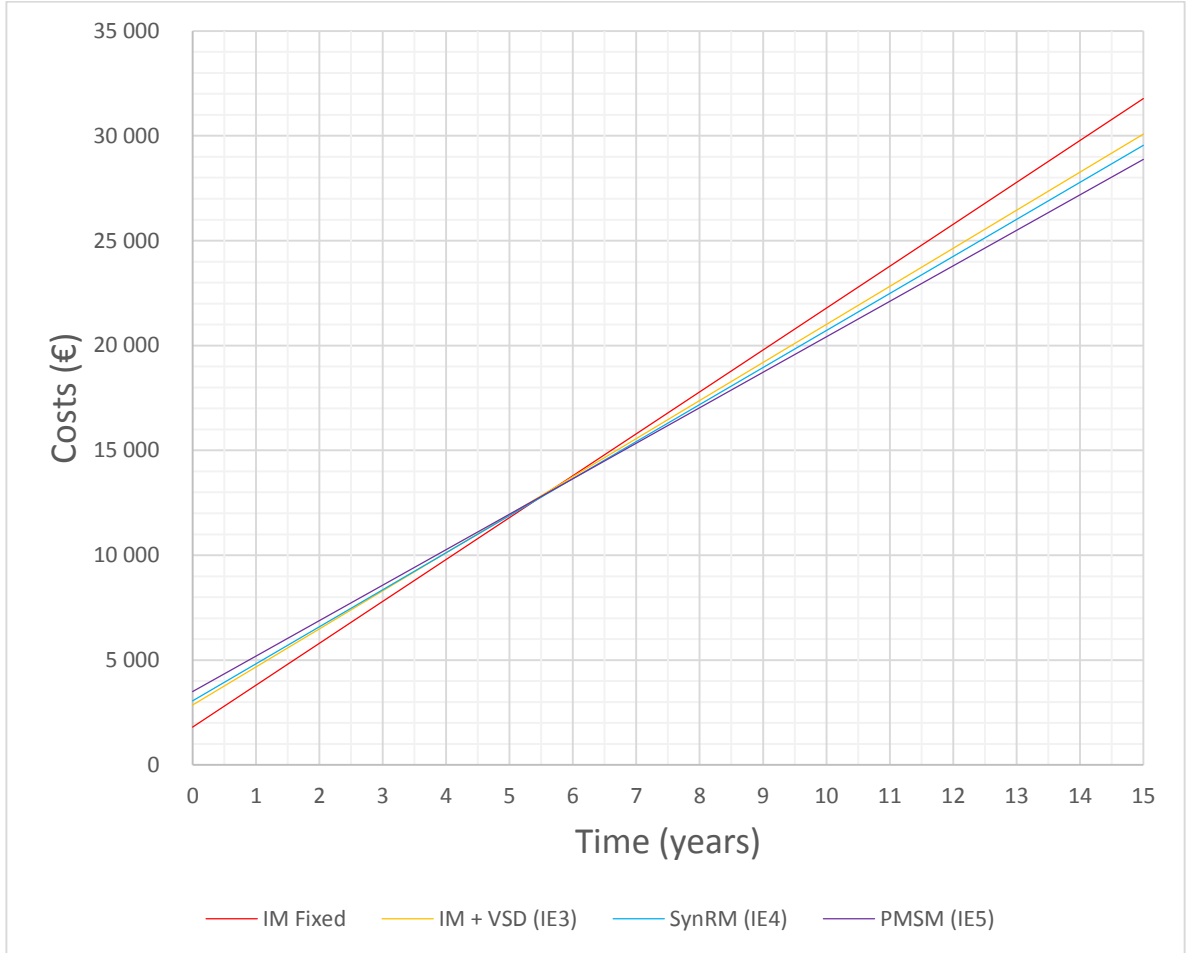
Fig 4.1 Motor efficiency classes and their annual energy consumptions.

The first thing to notice is that the IM fixed investment costs are smaller compared to the other motors, but through a long period of time is the less reliable option since its energy costs difference increases considerably. On the other hand, a PMSM considered as IE5 has the higher investment costs but the payback time compared to the IM running a VSD is about 5.5 years. The same IE5 motor becomes more reliable compared to the IE4 SynRM after 6 years. An IE4 motor payback time is around 5 years compared to the IE3 induction motor.

Now in terms of economy, another variable to analyze could be the Internal Rate of Return (IRR), which can be estimated considering the variation of electricity prices in different years [40] and gives the idea whenever a project is more reliable than other according to the investment costs and the profit which varies year by year. In our case, those "projects" will be simply the motors considering the aspects from the purchase price to the energy costs through the years. IRR is calculated as a percentage where the higher value means the more reliable a project is.

Considering a period of 10 years with the data taken from [40], purchase prices from Table 3.1 and energy costs from Table 3.7, the estimated IRR indicates that, compared to the IM with VSD, the SynRM resulting value of 27% makes it more reliable than the PMSM with a 20% IRR. So the SynRM would provide a better chance of strong growth.

Chapter 5

5 Conclusions

The implementation of a variable speed drive was proven to bring a considerable energy saving potential for pumping systems while using a SynRM (considered as an IE4 class), bringing a 2% higher efficiency than the IM (IE3 class). SynRM was also more suitable for pumping applications because it is designed to work with a VSD and due to the frequency changes, the variation of reactances affect the behavior of the IM which needs to be adapted in order to work with a VSD.

It was shown that the effect of reducing the speed leads to a very large reduction in power consumption. After solving the needed speeds and pump shaft power to realize the best efficiency points of the pump, at full flow rate, the energy consumption was reduced by 15% from the 15 kW studied motor and the most remarkable difference was found at half flow rate, reducing the power consumption around 60%.

Measurements and tests were successfully performed inside LUT laboratories, comparing the efficiency results from the SynRM manufacturer's declaration with the obtained ones bringing less than 1% difference that can be justified according to the given tolerances from the motor data sheet.

Efficiency maps were obtained representing the SynRM package efficiency indicating that the pump only requires about 88% of the motor nominal torque according to the operating points using the load profile for closed loop systems which translates into a lower energy consumption. Efficiency maps for the IM and PMSM are also shown where the later one

data was obtained using FEM and simulations. The PMSM fulfilled the characteristics of the higher efficiency class (IE5) contemplated at the moment, bringing the higher efficiency within the three motor types.

The effect of dimensioning our 15 kW SynRM motor to a 18.5 kW one results in lower load torque of about 70% at the maximum efficiency point and the efficiency itself is close to the 92% curve, this could mean some advantages to be reflected into energy savings in a long term period depending on the purchase price of each motor.

Further research can be done including a PMASynRM for comparison on the study of the energy consumption whenever the commercial data, characteristics and purchase prices for this type of motor are available.

IM investment costs are smaller compared to the other motors, but the overall energy costs on a long period make it the less reliable option since its difference increases considerably. PMSM has the higher investment costs but the payback time compared to the IM is about 5.5 years. An IE4 motor payback time is around 5 years compared to the IE3 induction motor. The same PMSM motor becomes more reliable compared to the SynRM after 6 years.

Chapter 6

6 Summary

The majority of the motor electricity consumption takes place in pumping, fan and compressor systems, representing more than 60% in the industrial sector and more than 80% in the services sector. Improvements in the system components, design and overall fluid system operation can be done in order to increase the system energy efficiency. Of these options, especially the use of variable-speed operation often provides the largest energy saving potential for different fluid handling systems that further on can be translated into Mtons reduction of CO_2 emissions.

To achieve the sought improvements in the system components, some standards and regulations are being adopted for fluid handling systems, like the Minimum Efficiency Index (MEI) that limits the water pumps with less efficiency out of the European market on the coming years. However, the European Association of Pump Manufacturers (Europump) is aiming for a greater energy saving action by using a methodology to calculate the Energy Efficiency Index (EEI) for the whole pumping system, including also the integrated pump units such as circulator pumps.

Electric motors have a corresponding efficiency-based classification that in European Union is based on International Efficiency (IE) classes. In order to introduce higher efficiency motors into the market. Classes are labeled from IE1 to IE5 (indicative in the latest revision of IEC 60034-30 standard).

This thesis studies the efficiency characteristics of existing electric motor types to determine the effects of motor efficiency (IE class), motor sizing and changes in the electricity price on the resulting energy consumption and costs in a pumping system. The study is realized by determining the efficiency maps of 15 kW IM, SynRM and PMSM in the context of a pumping system operating in the closed loop configurations.

References

[1] *Market transformation of energy-efficient motor technologies in the EU.* **de Almeida A., Fonseca P., Falkner H. and Bertoldi P. 2003.** 6, s.l. : Energy Policy, 2003, Vol. 31.

[2] *Implementing Directive 2009/125/EC of the European Parliament and of the Council with regard to ecodesign requirements for water pumps.* **European Commission. 2012.** 547, s.l. : Official Journal of the European Union, 2012.

[3] **European Association of Pump Manufacturers. 2013.** Extended product approach for pumps. Brussels : Europump, 2013.

[4] **Modern comfort. Grundfos. 2012.** *http://moderncomfort.grundfos.com/int/heating-hot-water/heating/magna3/#/features.* [Online]

[5] **Xylem. Flygt Experior. 2014**. *http://www.flygt.com/en-us/Pumping/Experior/Pages/default.aspx.* [Online]

[6] **European Commission. 2003.** *European Guide to Pump Efficiency for Single Stage Centrifugal Pumps.* Brussels : Europump, 2003.

[7] **Solovyeva, Elena. 2013.** *Mathematical Models and Stability Analysis of Induction Motors under Sudden Changes of Load.* Jyväskylä : Jyväskylä University Printing House, 2013. ISBN 978-951-39-5521-2

[8] **Juha Pyrhönen, Tapani Jokinen, Valéria Hrabovcová. 2008.** *Design of Rotating Electrical Machines.* Lappeenranta : John Wiley & Sons, 2008. ISBN: 978-0-470-69516-6

[9] **Azuara, Cosme Antonio. 2013.** *Accuracy Analysis of Frequency Converter Estimates in Diagnostic Applications.* Turku : s.n., 2013.

[10] **Heikkilä, Tanja. 2002.** *Permanent Magnet Synchronous Motor for Industrial Applications.* Stockholm : s.n., 2002. ISBN 951-764-699-2.

[11]   **Pyrhönen, Juha. 2010.** Electrical Drives course material. Lappeenranta : Department of Electrical Engineering, 2010.

[12]   **ABB Motors and Generators. 2013.** *IE4 synchronous reluctance motor and drive package for pump and fan applications.* s.l. : ABB, 2013.

[13]   **Europump; Hydraulic Institute. 2004.** Variable Speed Pumping a Guide to Successful Applications. s.l. : Europump, 2004.

[14]   **ABB Switzerland Ltd. 2007.** Motor bearings. Dättwil : ABB, 2007.

[15]   **Chapman, Stephen J. 1999.** *Electric Machinery Fundamentals.* 3rd. Boston : McGraw-Hill Science/Engineering/Math, 1999. ISBN:9780070119505.

[16]   *A Permanent Magnet-Assisted Synchronous Reluctance Motor.* **HIROSHI MURAKAMI, YUKIO HONDA, SHIGEO MORIMOTO, YOJI TAKEDA. 2003.** 4, Osaka : Electrical Engineering in Japan, 2003, Vol. 142.

[17]   **Liu, Tian-Hua. 2011.** [bok section] Moulay Tahar Lamchich. *Torque Control.* Rijeka, Croatia : InTech, 2011.

[18]   **Sulzer Pumps Ltd. 2014.** New Hygienic Injection Pump Series. Winterthur, Switzerland : Sulzer, 2014.

[19]   **Nidec Motor Corporation. 2013.** TechDocs: Product Facts: Modern Aluminum Alloys. *Nidec Motor Corporation website.* [Online] 2013. http://www.usmotors.com/TechDocs/ProFacts/Aluminum-Alloys.aspx.

[20]   **Moghaddam, Reza - Rajabi. 2011.** Synchronous Reluctance Machine (SynRM) in Variable Speed Drives (VSD) Applications. Stockholm : The Royal Institute of Technology, 2011. ISBN 978-91-7415-972-1.

[21]   *A Low-Cost and Efficient Permanent-Magnet-Assisted Synchronous Reluctance Motor Drive.* **Peyman Niazi, Hamid A. Toliyat, Dal-Ho Cheong, Jung-Chul Kim. 2007.** Issue 2: IEEE, 2007, Volume 43.

[22]   *Analysis of Hybrid Permanent Magnet Assisted Synchronous Reluctance Motor for Compressor.* **Yu, Minghu. 2013.** Busan, Korea : Guangdong Meizhi Compressor Limited, 2013.

[23]   **ABB Group. 2012.** *SynRM motor and drive package, Motor Summit.* s.l. : ABB, 2012.

[24]   *On-line Parameter Identification Scheme for Vector Controlled Drive of Synchronous Reluctance Motor without Shaft Encoder.* **Mona Moussa, Yasser Dessouky. 2013.** Alexandria, Egypt : Global Advanced Research Journals, 2013, Vol. 2. ISSN: 2315-5124.

[25]   *Performance Comparison of Permanent Magnet Synchronous Motor and Induction Motor for Cooling Tower Application.* **H.K.Patel, Raj Nagarsheth, Sharang Parnerkar. 2012.** 8, Gujarat, India : International Journal of Emerging Technology and Advanced Engineering, 2012, Vol. 2. ISSN 2250-2459.

[26]   *Comparison and design of different electrical machine types regarding their applicability in hybrid electrical vehicles.* **Thomas Finken, Matthias Felden, Kay Hameyer. 2008.** Aachen, Germany : RWTH Aachen University, 2008.

[27]   *Design and Comparison of an Optimized Permanent Magnet-Assisted Synchronous Reluctance Motor (PMa-SynRM) with an Induction Motor with Identical NEMA Frame Stators.* **Robert Vartanian, Hamid A. Toliyat. 2009.** Texas : IEEE, 2009. 978-1-4244-3439-8.

[28]   **ABB. 2014.** IEC 60034-30-1 standard on efficiency classes for low voltage AC motors. *Technical data.* s.l. : ABB, 2014.

[29]   **Lenze Ltd. 2013.** *Using energy-efficient electric Motors. Meeting the International Energy Directives.* Bedford : Lenze Ltd, 2013.

[30]   **ABB. 2014.** *IE5 Ultra premium efficiency without rare earth magnets.* s.l. : ABB, 2014.

[31]   **KSB. 2013.** *KSB SuPremE – The World's Most Efficient Magnet-less Pump Motor.* Frankenthal : KSB Aktiengesellschaft, 2013.

[32]   **ABB. 2013.** *ACS850-04 Drive Modules Hardware Manual.* 2013. 3AUA0000045496 Rev F.

[33]   *Reading Centrifugal Pump Curves.* **Satterfield, Zane. 2013.** 1, West Virginia : THE NATIONAL ENVIRONMENTAL SERVICES CENTER, 2013, Vol. 12. DWFSOM155DL

[34]   **United Nations Environment Programme. 2006.** Energy Efficiency Guide for Industry in Asia. *Energy Efficiency Asia.* [Online] 2006. www.energyefficiencyasia.org.

[35]   *The Motor Guide- basic technical The Motor Guide- basic technical motors.* **ABB. 2005.** 2nd edition, s.l. : ABB LV Motors, 2005. ISBN 952-91-0728-5

[36]   *A Modified Approach to Induction Motor Stator Voltage and Frequency Control. .* **Cosmas Uchenna Ogbuka, Marcel U. Agu. 2009.** 1, Nsukka, Nigeria : The Pacific Journal of Science and Technology , 2009, Osa/vuosik. 10.

[37]   **Sebastian Lang, Gerhard Ludwig, Peter F. Pelz, Bernd Stoffel. 2013.** *General Methodologies of Determining the Energy-Efficiency-Index of Pump Units in the Frame of the Extended Product Approach.* s.l. : Technische Universitat Darmstadt, 2013.

[38]   *Comparison of electric motor types for realising an energy efficient pumping system.* **Ahonen, Tero;Tamminen, Jussi; Montonen, Juho. 2014.** Lappeenranta, Finland : Lappeenranta University of Technology, 2014.

[39]   *Beyond Induction Motors—Technology Trends to Move Up Efficiency.* **Almeida, Aníbal;Ferreira, Fernando ja Ge, Baoming. 2014.** s.l. : IEEE TRANSACTIONS ON INDUSTRY APPLICATIONS, 2014, Volume 50, No.3.

[40]   **2015.** Eurostat. *Electricity prices by type of user.* [Online] 28. 09 2015. [Referenced: 07.   12   2015.]

http://ec.europa.eu/eurostat/tgm/table.do?tab=table&init=1&plugin=1&language=en&pcode=ten00117.